AUSTRALIAN NATIONAL ANTARCTIC RESEARCH EXPEDITIONS

A N A R E

R E S E A R C H

N O T E S

56

Diurnal, seasonal and storm-time variability of the total electron content of the ionosphere north of Macquarie Island

M. Craven
E.A. Essex

ANTARCTIC DIVISION
DEPARTMENT OF THE ARTS, SPORTS, THE ENVIRONMENT, TOURISM AND TERRITORIES

ANARE RESEARCH NOTES (ISSN 0729-6533)

This series allows rapid publication in a wide range of disciplines. Copies of this and other ANARE Research Notes are available from the Antarctic Division. Any person who has participated in Australian National Antarctic Research Expeditions is invited to publish through this series. Before submitting manuscripts authors should obtain a style guide from:

The Publications Office
Antarctic Division
Channel Highway
Kingston
Tasmania 7150
Australia.

Published December 1987
ISBN: 0 642 12296 2

CONTENTS

FIGURES

TABLES

DIURNAL, SEASONAL, AND STORM-TIME VARIABILITY OF THE TOTAL ELECTRON CONTENT OF THE IONOSPHERE NORTH OF MACQUARIE ISLAND

by

M. Craven and E.A. Essex

Division of Theoretical and Space Physics
La Trobe University
Bundoora, Victoria, Australia

ABSTRACT

Measurements taken near solar minimum of the total electron content (TEC) of the ionosphere equatorward of Macquarie Island (54.5°S, 158.9°E), using the Faraday rotation techniques are presented. The data collected indicate that the peak in daytime TEC maximises around late autumn, progressively decreases through winter to spring, and gradually recovers with the onset of summer. The morning post-sunrise build up phase of TEC becomes progressively less uniform from winter through summer, whilst the post-sunset TEC decay phase is often disrupted, during all seasons, by the onset of geomagnetic disturbances and/or the passage of the ionospheric trough. Magnetic storm events are often accompanied by a large increase in TEC lasting several hours, with increased geomagnetic activity on successive evenings, and a general reduction of daytime TEC levels during the storm recovery phase over 2-3 days. The largest percentage increases in TEC generally occur around the time of the minimum value of the Dst-index.

1. INTRODUCTION

The Faraday rotation technique for measurement of total electron content (TEC) has been described in Lambert et al. (1986). A brief outline will be given in this Research Note for completeness. Lambert el al. (1986), whilst presenting relative measurements of TEC only, suggested possible means of converting the data to absolute figures. The results of this extended analysis are presented here, and the data displayed in a number of different formats to highlight various aspects. Reference should be made to Lambert el al. (1986) for a description of the experimental setup and file handling procedures.

2. THE FARADAY ROTATION TECHNIQUE

Essentially the phenomenon of Faraday rotation arises from the anisotropy imparted upon electromagnetic waves as they pass through the ionosphere, by the presence of the Earth's magnetic field. A plane polarised wave is split into two characteristic waves, the ordinary and extraordinary magnetoionic components, as it propagates through the ionosphere. Since the two components travel with different phase velocities, the plane of polarisation (due to their vector sum) rotates continuously along any ionised parts of the transmission path. Thus the total signal rotation from a geostationary satellite source to the receiver, is a measure of the TEC along the entire path between the two.

The derived relationship between Faraday rotation and TEC using the Appleton equations (Davies 1969) takes the mathematical form:

$$\Omega = \frac{K}{f^2} \int_0^{h_s} N(h)\, B(h) \cos\theta \sec\phi \, dh \qquad (1)$$

where:

- Ω = Faraday rotation in radians
- K = 2.365×10^4
- f = wave frequency in Hz
- $N(h)$ = altitude dependent electron density in elm^{-3}
- $B(h)$ = altitude dependent magnetic field strength in Tesla
- θ = angle between ray path and $B(h)$
- ϕ = zenith angle of ray path
- h_s = altitude of satellite in m
- h = vertical distance in m

TEC could be calculated directly from equation 1 if the integral were analytically tractable. Since it involves altitude dependent quantities a full analysis would require the use of a suitable ionospheric model to substitute into equation 1. The bulk of the Faraday rotation suffered by a propagating wave occurs where the electron concentration (N(h)) is greatest, around the F2-level of the ionosphere. This allows use of an approximation which draws the magnetic field contribution out of the integral in the form of the Faraday M-factor:

M = 'average value' of $B(h) \cos\theta \sec\phi$ at 400 km altitude

so that:

$$\Omega = \frac{KM}{f^2} \int_0^{h_s} N(h)\, dh \qquad (2)$$

and:

$$TEC = \int_0^{h_s} N(h)\, dh \quad \text{by definition}$$

The Faraday M-factor, M, is then evaluated from the values of B(h) (= B_o), θ, and φ at the F2-peak in the ionosphere (Figure 1). Called the ionospheric point, this marks the spot where the source-receiver propagation path intersects the ionosphere at an altitude of 400 km. The latitude and longitude of the point on the Earth's surface vertically below is labelled the sub-ionospheric point (SIP).

Elementary spherical trigonometry is then used to determine the co-ordinates of the SIP from a knowledge of the satellite and receiver locations. For a true geostationary orbit this calculation need be made but once. Such was the case for the bulk of the Faraday measurements discussed here involving use of the signal from the near geostationary satellite ETS-2. During equinoctial power conservation shut-down procedures on board ETS-2, transmissions were accepted from the satellite ATS-1 which is somewhat less than geostationary, suffering a periodic oscillation approximately 11° either side of the equator per sidereal day. It was therefore necessary to adjust the M-factor to account for this movement in the similarly periodic motion of the ionospheric point for the ATS-1 data (Table 1).

Once the ionospheric point has been properly determined, the Faraday M-factor is evaluated using the magnitude and direction of the Earth's magnetic field, at the ionospheric point, as derived from the International Geophysical Reference Field (IGRF) spherical harmonic models (Zmuda 1971, Peddie 1982).

3. RELATIVE TO ABSOLUTE TEC

The receiver can only assign a value in the range 0-π for the Faraday rotation Ω. It is therefore incapable of discriminating between signals which have undergone multiple complete rotations : Ω + nπ. For this reason the article by Lambert et al. (1986) could provide only plots of the relative polarisation of the signal, and hence, relative TEC. As indicated there, Smith (1971) has suggested a means for removal of the nπ-ambiguity in measurements of TEC. This involves use of the ionospheric F2-layer critical frequency foF2. This value is directly related to the maximum electron density of the F2-layer.

Smith (1971) shows that the total Faraday rotation is proportional to the square of the foF2-value, with a proportionality factor, S, which is affected by the shape of the electron density profile:

$$\Omega = S\,(foF2)^2 \qquad (3)$$

Providing this relation holds, then a plot of a series of relative TEC measurements, Ω, against corresponding values of $(foF2)^2$ will yield a straight line, of gradient equal to S. The intercept on the Ω-axis will yield the '$n\pi$' error between the relative and absolute TEC measurements. Since the relative polarisation, α, between transmit and receive antennae is not known, the measured intercept will in fact be $(n\pi-\alpha)$.

The shape of the electron density profile, and hence the factor S, has a pronounced diurnal variation, rendering it invalid to plot Ω versus $(foF2)^2$ for consecutive observations throughout a single day. However, for measurements taken at the same time on successive days the electron density profile shows little change (so S remains constant), provided the period over which the observations are made is small enough that seasonal variability effects remain negligible. This was the method adopted for the results reported here.

Since the TEC information derived from this analysis actually applies to the ionosphere at the location of the SIP, the foF2's required for the intercept evaluation should ideally also be measured at the SIP. In the case of the current research, the locations of the SIP's for transmission from ETS-2, and ATS-1 to Macquarie Island, lie in open ocean approximately midway between Macquarie Island and Hobart (Figure 2). As an approximation to the ionospheric conditions at the SIP, the foF2-values of Hobart and Macquarie Island were averaged. Smith (1971) suggested that the intercept technique is best applied when the TEC is close to its diurnal minimum, that is pre-dawn, 0400 LT. However foF2 can rarely be obtained from Macquarie Island ionograms at that time due to the common occurrence of auroral activity producing absorption of the ionosonde signal. The analysis was shifted to around noon, 1200 LT when a much greater abundance of foF2 data was available from both stations. This method has been adopted by Checcacci and Giorgio (1976).

Figure 3 presents plots of Ω vs. $(foF2)^2$ for two of the observation periods analysed. Linear regression lines using either variable as the independent one, and the mean of these two as per Checcacci and Giorgio (1976), are drawn in to indicate the determination of the intercept, and the likely error involved. Points plotted directly on the Ω-axis indicate days when either the Macquarie Island (usually) or Hobart foF2-value was not available.

Deduction of the measured intercept from the raw data for each period of observation, together with application of the calculated Faraday M-factor, then allows absolute TEC figures to be established. One final step, to clean up the data, involved removal by hand of spurious satellite signals which appear as noise spikes on the data approximately 110 minutes (orbital period) apart (Figure 4).

4. DATA AND DISCUSSION

A total of 247 days absolute TEC data were determined covering the period May 1984 to Jan 1985, yielding a seasonal coverage extending from late-autumn to mid-summer. Pseudo-three-dimensional plots of all the data are given in Figure 5, indicating the daily variation in TEC on a monthly basis. Night-time (0800-1600 UT) disturbance activity is clearly evident, as is the uniformity of the morning build-up of TEC, from May through August in particular.

Monthly averages, and their corresponding standard deviations, were calculated at fifteen minute intervals (Figure 6). As a measure of the day-to-day variability of the figures, the percentage ratio of the standard deviation to the average TEC is also shown.

The daytime TEC peak is maximum in May-June (late autumn-winter, no March-April data are available) at around 15 TEC units (1 TEC unit = 10^{16} elm^{-2}). This descends through July-August to an October (spring) minimum near 10 TEC units, then gradually recovering by December-January (mid-summer) to levels around 12.5 TEC units.

By way of comparison, Soicher (1986) reports for 1976-77 data that average monthly TEC values were always below 15 TEC units in a Northern Hemisphere study from Anchorage, Alaska, for a SIP at 52.1°N, 131.0°W, L-shell value 3.35 (c.f. SIP for ETS-2 to Macquarie Island at 48.45°S, 152.89°E, L-shell value close to 4.0). He found a seasonal variability wherein the maximum daytime peak occurred in April (spring) with progressively lower values through August (late summer), October (autumn) to December (winter) respectively.

Soicher (1986) results were obtained over a period 10-18 months following the March 1976 solar minimum (between cycles 20-21), whilst the results presented here were gathered some 10-20 months prior to the September 1986 solar minimum.

Soicher (1986) also contrasted his subauroral zone figures with those of a mid-latitude location with an SIP at 36.5°N, 76.9°W, using a receiver at Fort Monmouth. Those figures indicate the daytime TEC maximum peaking in August (summer), being somewhat lower in December (winter), and lower still during the equinoctial periods. A number of complex mechanisms and effects are obviously in play here including the location of the mid-latitude ionospheric trough region.

In agreement with Soicher (1986) the authors found that the daytime day-to-day variability, as measured by the ratio of the standard deviation to the average TEC values, shows no significant seasonal variation. This ratio is always less than 25% during the day, and usually greater than 25% (often exceeding 50%) during the night.

Some mid-latitude Southern Hemisphere data have been gathered by Titheridge (1966) using a receiver located at Auckland, New Zealand (36.51°S, 174.45°E) from June 1965 to April 1966, again near a solar cycle minimum. Titheridge found a diurnal range whereby the ratio of the average daytime maximum TEC level (of the order of 9 TEC units) to the average night-time minimum was around 2:1 in June (winter), increasing to just above 3:1 (with average peak TEC levels of the order of 15 TEC units) by December (summer). In contrast the subauroral zone figures presented here indicate a diurnal range of 5:1 for June (winter), decreasing to around 3:1 by December (summer). Titheridge (1966) points out that the normal seasonal change he measured is for summer daytime TEC levels to be 80% larger than those for winter, and that the cosine of the solar zenith angle is similarly 82% greater in summer than in winter at Auckland. His seasonal change in TEC is therefore consistent with seasonal solar EUV (extreme ultra-violet) and UV ionisation rates. As Soicher (1986) indicates, the magnetosphere-ionosphere interaction is a further dynamic force in addition to solar ionisation at higher latitudes, so the behaviour of the ionosphere at L = 4 equatorward of Macquarie Island could be expected to show marked differences with that at mid-latitudes.

One further complementary way of representing the data is with the use of iso-TEC contours as a function of universal time and day of month (Soicher 1986) as shown in Figure 7. The day-to-day uniformity of the morning build-up phase of TEC following sunrise is clearly evident in the quasi-parallel contours between 20-24 UT from May-October. As the summer months approach this feature is less evident (17-21 UT). The evening decay of TEC also displays a fair degree of day-to-day consistency.

5. MAGNETIC STORM EVENTS

The ionospheric F2-layer changes its density and height during magnetic storms (Matsushita 1959). Faraday rotation measurements of TEC can be used to show that not only does a redistribution of ionisation take place, but also that genuine changes occur in the total amount of ionisation present in the ionosphere. Ionospheric storms are complicated by diurnal, seasonal, and latitudinal controls, as well as the severity of the particular geomagnetic storm causing them (Martyn 1953, Matsushita 1959, Jones 1971, Mendillo 1973, Essex 1986), and other effects such as atmospheric composition, ionospheric electric fields, and energy deposition regions.

The type of ionospheric response to the magnetic storm falls into three basic categories where the TEC changes adopt the following patterns: (1) an increase in TEC for a couple of hours followed by a decrease from which it takes several days to recover, (2) no positive phase, the TEC decreasing immediately, or (3) the positive phase being delayed until the afternoon of the following day (Martyn 1953, Mendillo 1973).

Jones (1971) defines an 'S-event' in terms of the geomagnetic storm-time disturbance parameter, the equatorial Dst (H) index. An S-event is said to occur when Dst changes from a positive value through zero to a negative value of less than 20 nT within a few hours. The S-event starts when Dst goes through zero, and ends when it reaches its most negative value. Jones (1971) found that increases in TEC during storms were always associated with S-events, predominantly toward the end of the event, provided the S-event partly included the period 08-12 LT. This local time dependence has also been noted by Martyn (1953), Matsushita (1959), Mendillo (1973) and Essex (1986).

Jones and Rishbeth (1971) suggest that the positive phase in the TEC results from an increased meridional neutral wind velocity due to atmospheric heating at auroral latitudes from enhanced electrojet currents. The meridional winds transport ionisation up the magnetic field lines to a region where the loss rate is lower. They suggest that this process will have a strong local time dependence. If heating occurs at night there will be very little effect on TEC since vertical drift merely retards the slow loss of ionisation. Around sunrise the TEC is dominated by the rapid solar radiation production rate, so it will be insensitive to drift. After about 08 LT the reduction of effective loss rates due to the vertical drift allows large TEC increases to occur.

They further argue that this mechanism ceases either when heating effects stop or spread to all latitudes, so that temperature gradients are restored to normal. The negative phase of the ionospheric storm can then take maximum effect. The consensus of opinion is that the decrease in TEC is caused by an increase in the loss rate of O^+ ions due to an increase in the densities of molecular nitrogen and oxygen (Martyn 1953, Seaton 1956, Duncan 1969). Mendillo (1973) concludes 'that while most storms sooner or later produce depletions in the ionospheric electron densities, the occurrence of an initial positive phase depends on an interplay between the <u>strength and duration</u> of the mechanism which causes the enhancements near dusk and the <u>time-development and intensity</u> of the process which causes the atmospheric heating'. He also suggests that since auroral currents are important in determining the F-region response to geomagnetic storms, the auroral electrojet AE-indices may be of use in monitoring mid latitude ionospheric behaviour.

A number of S-events (Jones 1971) occurred during the TEC monitoring period considered here, May, 1984 to January 1985. These are plotted in Figure 8 in three parts. The top plot in each figure gives the average of 7 days pre-storm data (dotted line) against the TEC values for the succeeding 5 days of observation (solid line). The middle plot gives the percentage change in TEC throughout the period (maximum value allowed is 250%, to make the scale readable throughout the bulk of the period), and the lower plot gives the Dst index.

An average of one storm per month was obtained. For the events recorded, the TEC generally increased on successive nights following the storm commencement. Marked increases in the TEC are also present whenever the Dst-index approaches its minimum value. This occurs even if the Dst minimum occurs during the night for the SIP involved here, due to auroral substorm activity and its associated ionisation precipitation.

Magnetic storm parameters are given in Table 2 for the events plotted in Figure 8. Being close to a solar minimum during the period of these observations, only four storms achieved a minimum Dst below -100 nT, with a Kp of 8 being attained only once, on 16 November 1984 between 03-06 UT.

Only one S-event occurred during the daytime, that of the 23 June 1984 storm, reaching a minimum of only -55 nT at 24/0200 UT (close to SIP noon). A strong positive phase is evident, but since the magnetic storm itself had only a total duration of approximately 12 hours there is no evidence of a TEC decrease on successive days. No night-time auroral substorm activity evolves either, further emphasising the moderate nature of this event.

For all the other storms recorded here the Dst minima fell between 08-19 UT (approximately 1800-0500 LT), and the ionospheric storms ranged from strong daytime reductions in TEC for the 13-17 July event, to minor daytime enhancements in TEC for the 26-30 December and the 28-31 January events.

It is hoped to be able to follow up this data by comparing it with concurrent Northern Hemisphere measurements from Boston, and Japan. More importantly, the monthly average figures will be compared with those predicted by the International Reference Ionosphere, 1986. This future work will be continued by Essex.

Table 1. Summary of parameters for the geostationary satellites ETS-2 and ATS-1 transmissions to Macquarie Island. These are an update on figures provided by Lambert et al. (1986) through use of the latest IGRF magnetic models (Zmuda 1971, Peddie 1982).

Satellite	ETS-2	ATS-1
Position	130°E 0°S	166.5° ± 1.0°E 0° ± 11.4°S
Height	35 800 km	35 800 km
Frequency of beacon signal	136.112 MHz	137.35 MHz
Sub-ionospheric point	152.9°E 48.45°S	160.0° ± 0.8°E 48.0° ± 2.6°S
M.factor	6.570×10^{-5}T	7.3395×10^{-5}T (av.)
ΔTEC for π-rotation	3.75 TEC units	3.42 TEC units
Elevation from Macquarie Is	22.52°	27.66° ± 11.78°
Azimuth from Macquarie Is	325.86°	8.87° ± 1.21°

Table 2. Summary of storm-time parameters for each of the events plotted in Figure 8.

Date	Commencement Type	Commencement Time	Kp-Index Maximum	Kp-Index Time	DST(h) - Index Minimum	DST(h) - Index Time	End
23 June 1984	gradual	23/2000 UT	6-	24/00-03 UT	-55 nT	24/02 UT	24/08 UT
13 July 1984	S.C.	13/0601 UT	7	13/06-09 UT	-83 nT	13/15 UT	14/20 UT
			7	13/12-15 UT			
01 August 1984	gradual	01/0100 UT	7	01/03-06 UT	-107 nT	01/07 UT	02/16 UT
04 September 1984	S.C.	04/0745 UT	8-	04/15-18 UT	-120 nT	05/08 UT	05/24 UT
18 October 1984	gradual	18/0800 UT	7-	18/18-21 UT	-77 nT	18/18-19 UT	20/22 UT
			7-	19/18-21 UT			
			7-	20/18-21 UT			
14 November 1984	gradual	14/2300 UT	8	16/03-06 UT	-133 nT	16/08-09 UT	16/21 UT
26 December 1984	gradual	26/0800 UT	5+	28/06-09 UT	-48 nT	26/13 UT	29/06 UT
23 January 1985	S.C.	23/0806 UT	6-	23/03-06 UT	-39 nT	23/08 UT	23/24 UT
27 January 1985	gradual	27/1800 UT	6	28/15-18 UT	-117 nT	28/16 UT	29/01 UT

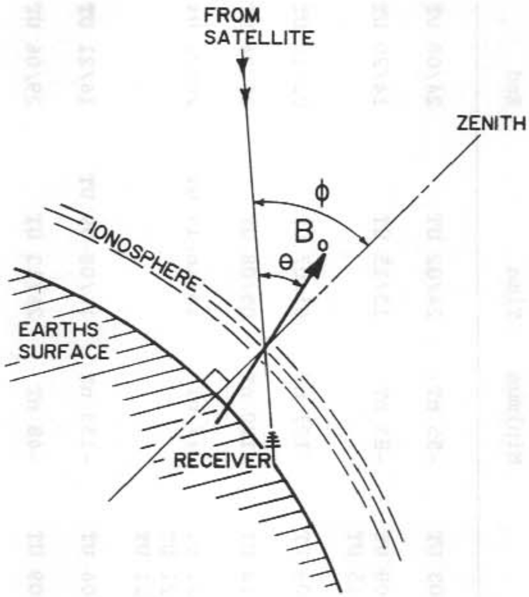

Figure 1. Geometry of the satellite to receiver ray path, and the relationship of the magnetic field at the ionospheric point (Lambert et al. 1986).

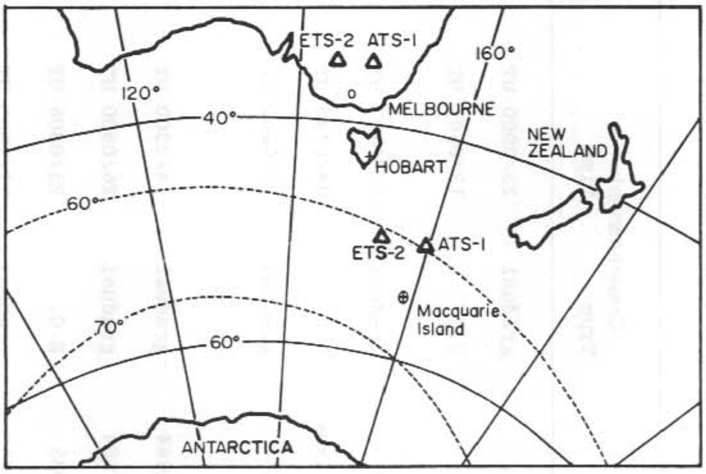

Figure 2. The approximate location of the sub-ionospheric points (SIP) from Macquarie Island for transmission from geostationary satellites ETS-2 and ATS-1 (Lambert et al. 1986). The dashed lines represent geomagnetic latitude. (SIP locations are also shown for another station located at Beveridge, near Melbourne.)

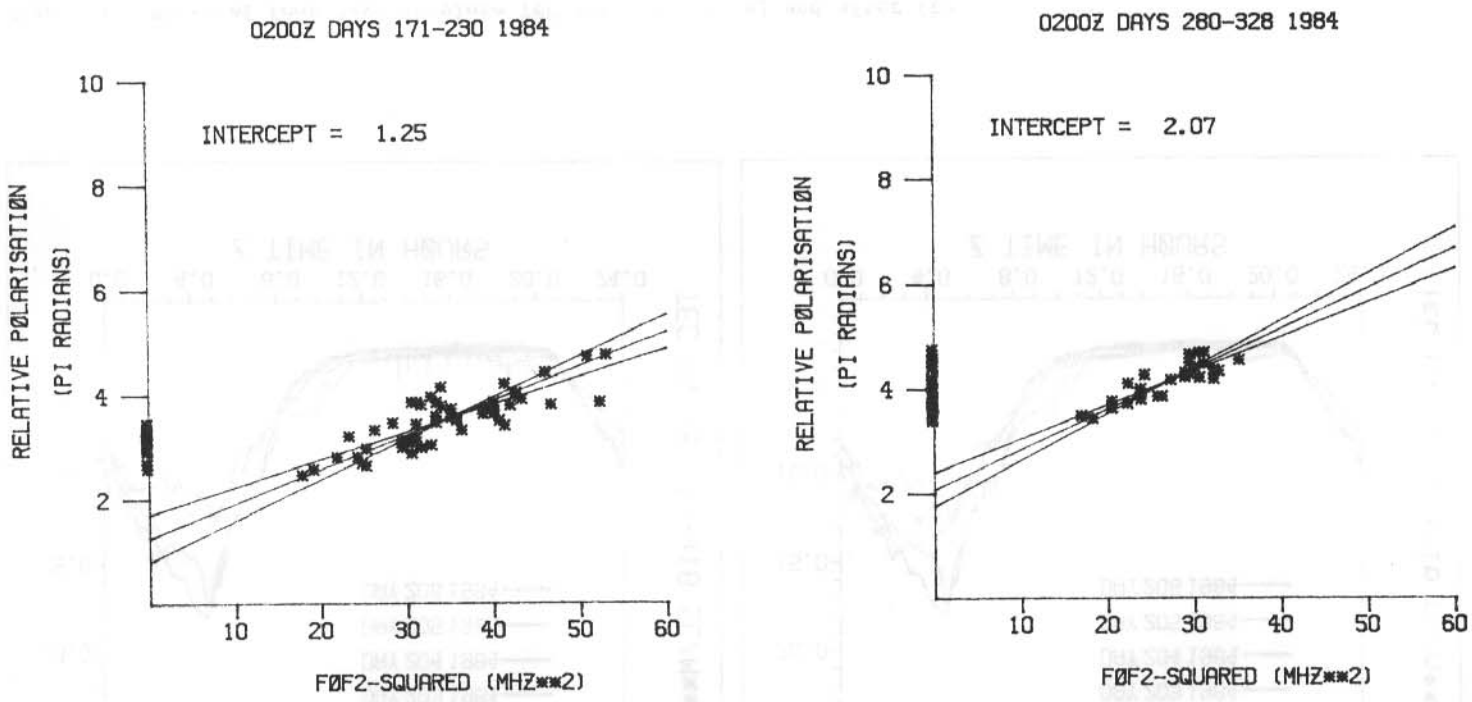

Figure 3. Plots of the phase of the Faraday rotation against the square of the F2-layer critical frequency in order to determine the total number of complete rotations suffered by the signal in its passage from satellite source to ground-based receiver. (These figures are relative to an arbitrary zero polarisation chosen so that the night-time minimum value is non-negative).

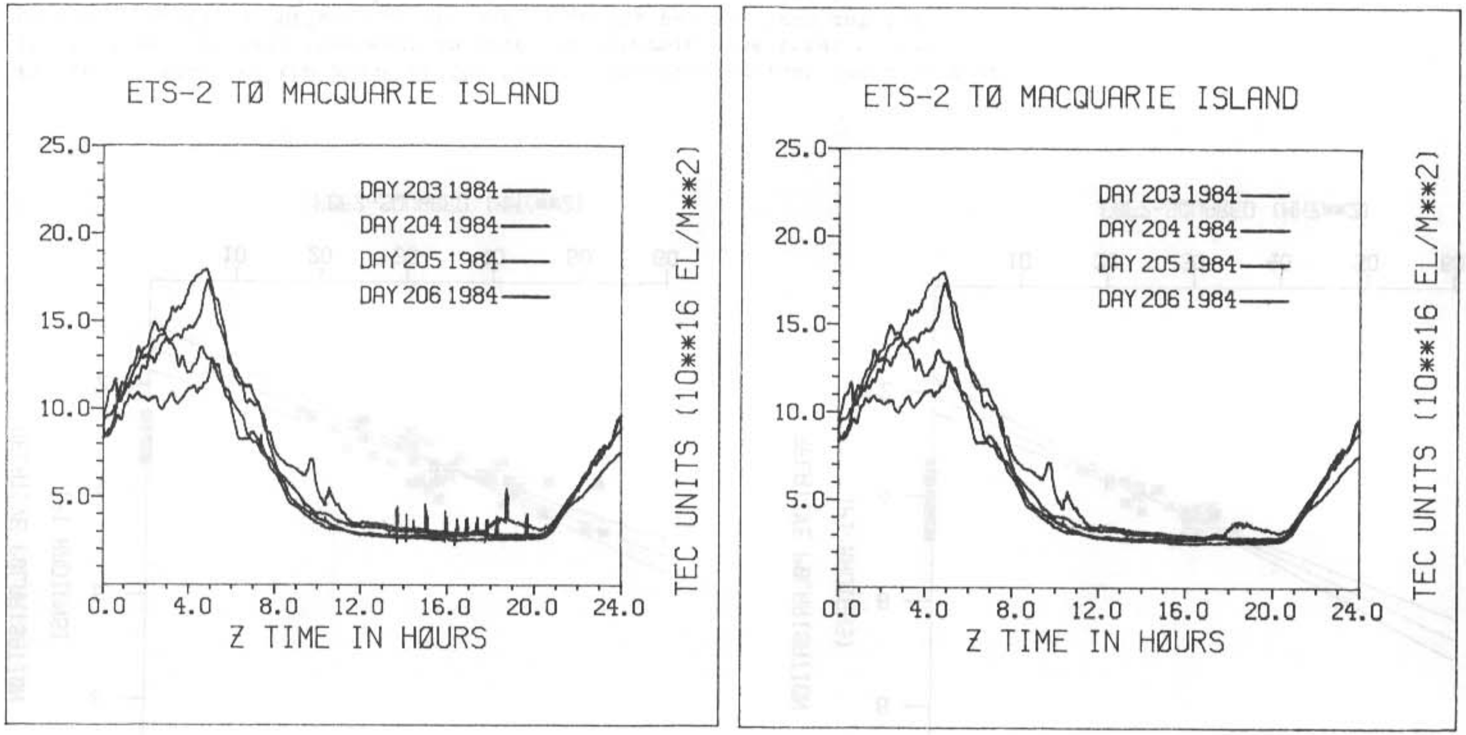

Figure 4. Plots of four days absolute TEC data before (a) and after (b) removal of spurious satellite interference signals (1 TEC unit = 10^{16} elm^{-2}) between 13-20 UT.

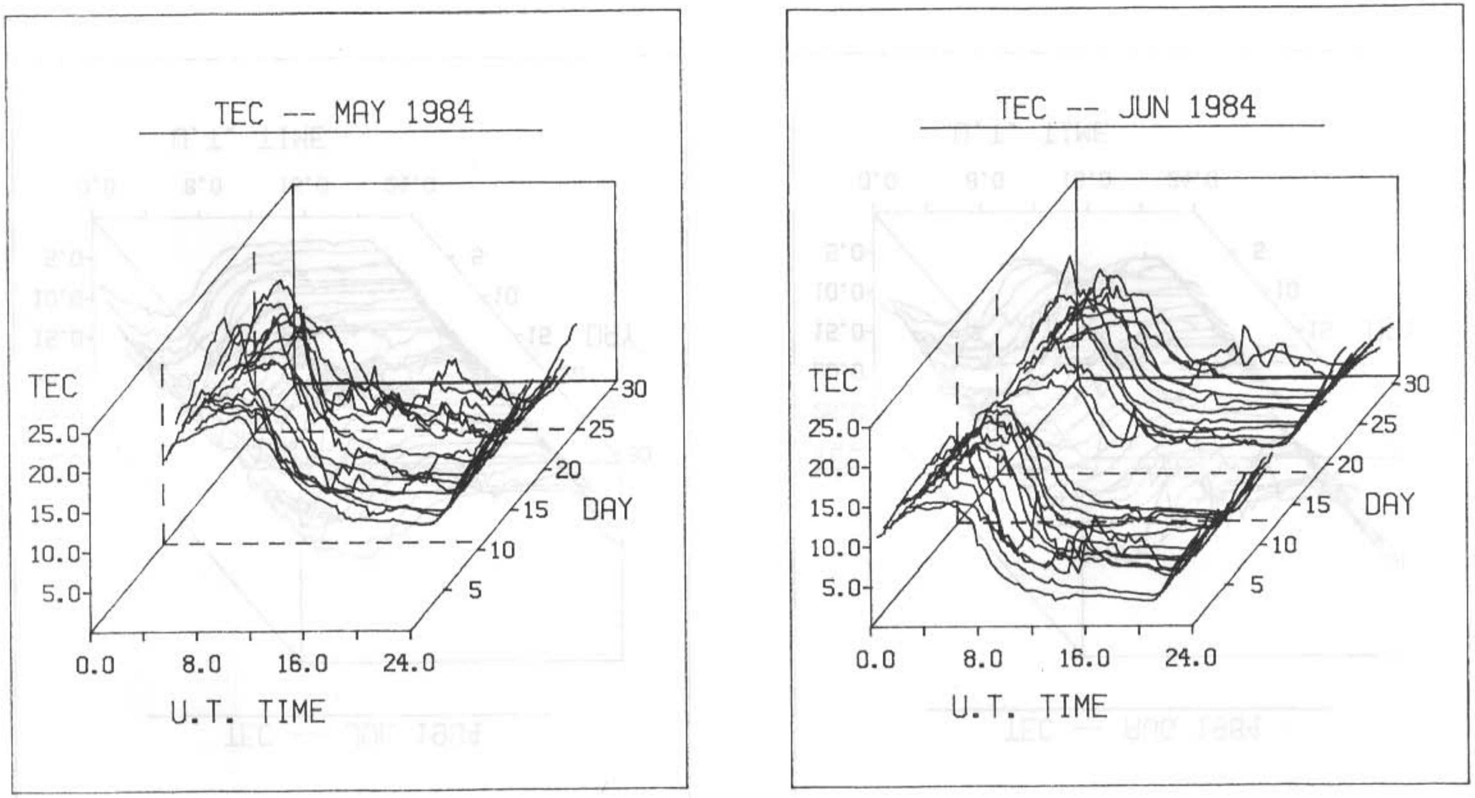

Figure 5. Three-dimensional monthly plots of daily absolute TEC for a Southern Hemisphere subauroral zone location, at a time near solar minimum. The 27-day recurrence of night-time substorm activity is clearly evident.

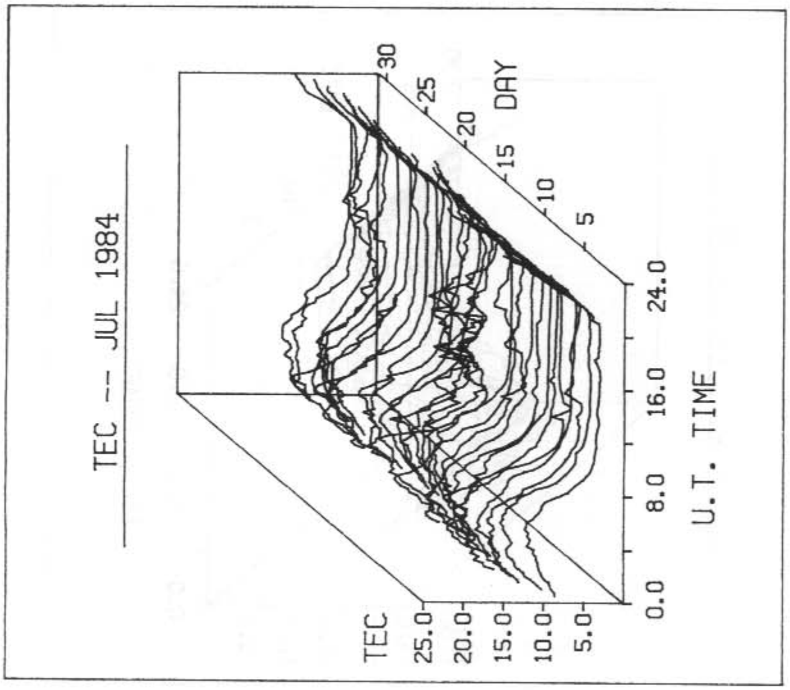
TEC -- JUL 1984
TEC
25.0
20.0
15.0
10.0
5.0
0.0
8.0
16.0
24.0
U.T. TIME
5
10
15
20
25
30
DAY

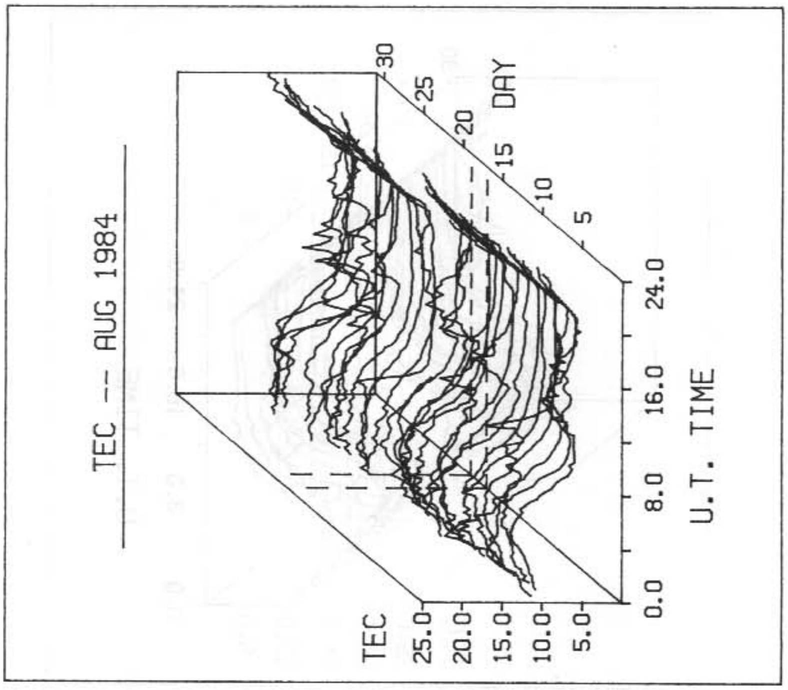
TEC -- AUG 1984
TEC
25.0
20.0
15.0
10.0
5.0
0.0
8.0
16.0
24.0
U.T. TIME
5
10
15
20
25
30
DAY

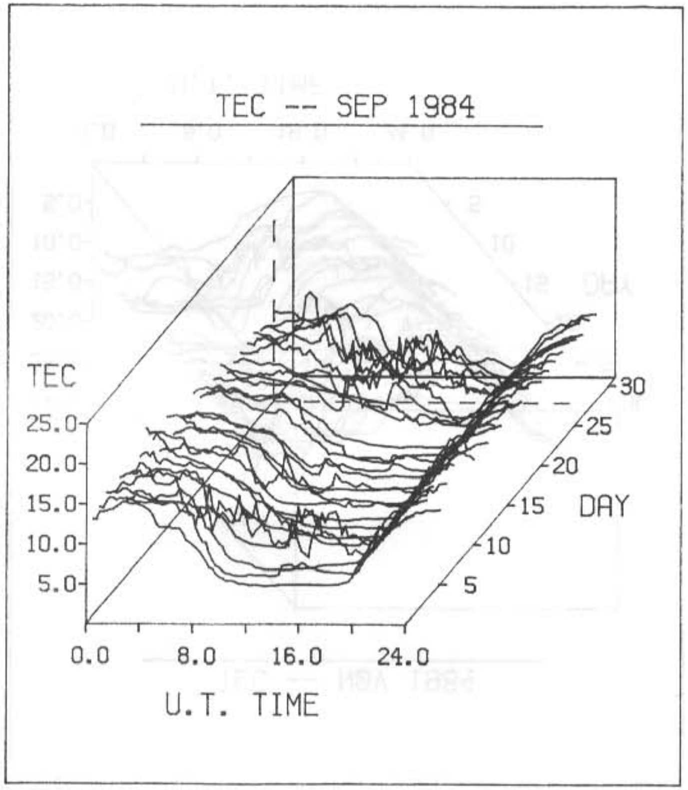
TEC -- SEP 1984
TEC
25.0
20.0
15.0
10.0
5.0
0.0
8.0
16.0
24.0
U.T. TIME
5
10
15
20
25
30
DAY

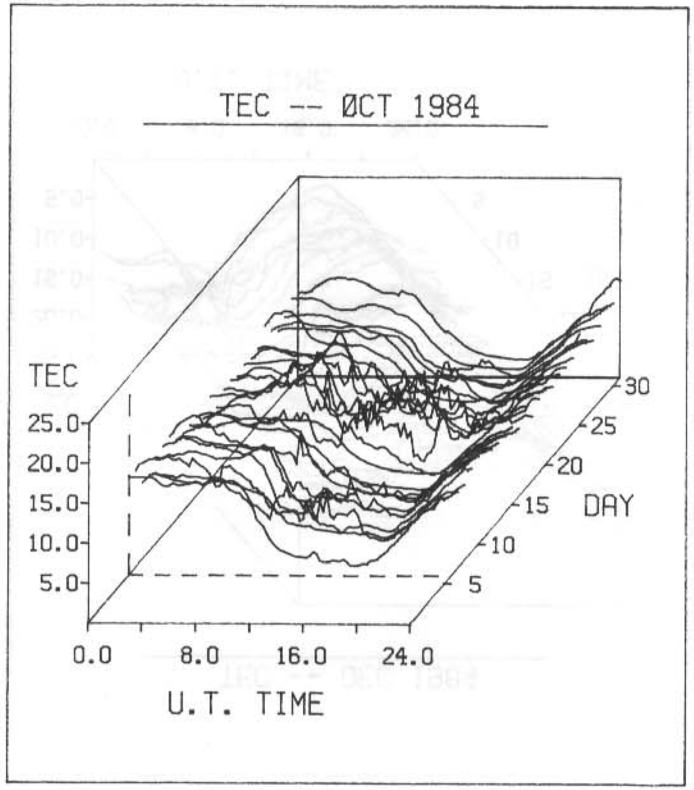
TEC -- ØCT 1984
TEC
25.0
20.0
15.0
10.0
5.0
0.0
8.0
16.0
24.0
U.T. TIME
5
10
15
20
25
30
DAY

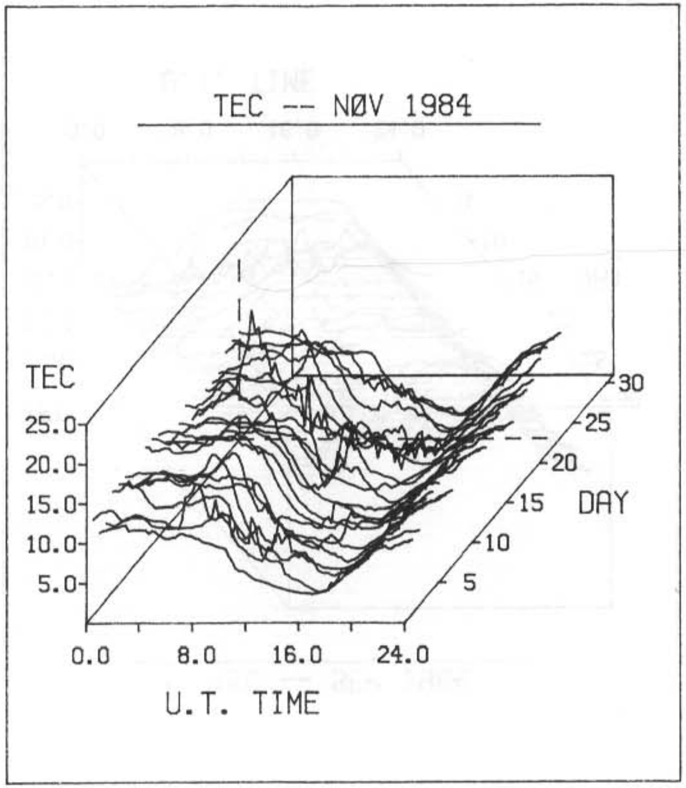
TEC -- NØV 1984
TEC
25.0
20.0
15.0
10.0
5.0
0.0
8.0
16.0
24.0
U.T. TIME
5
10
15
20
25
30
DAY

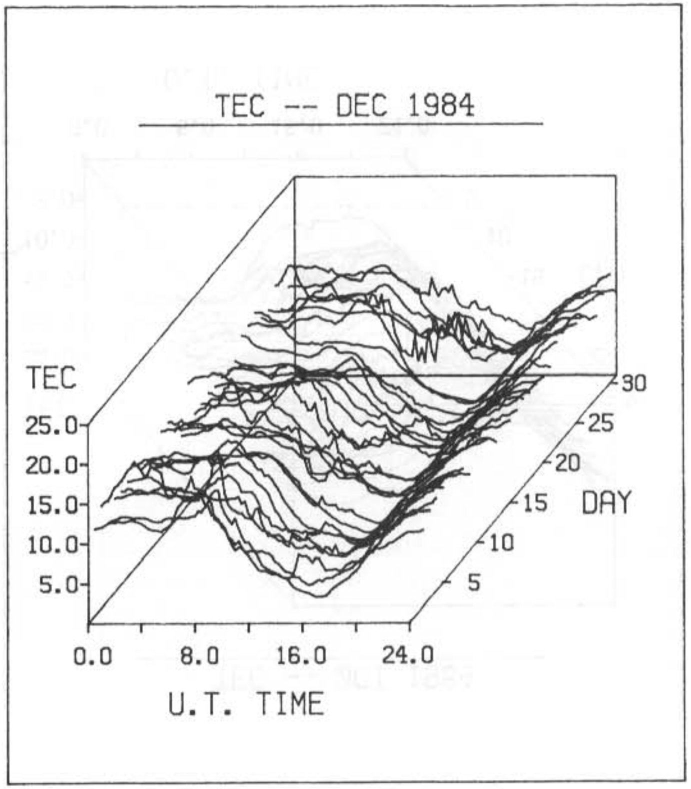
TEC -- DEC 1984
TEC
25.0
20.0
15.0
10.0
5.0
0.0
8.0
16.0
24.0
U.T. TIME
5
10
15
20
25
30
DAY

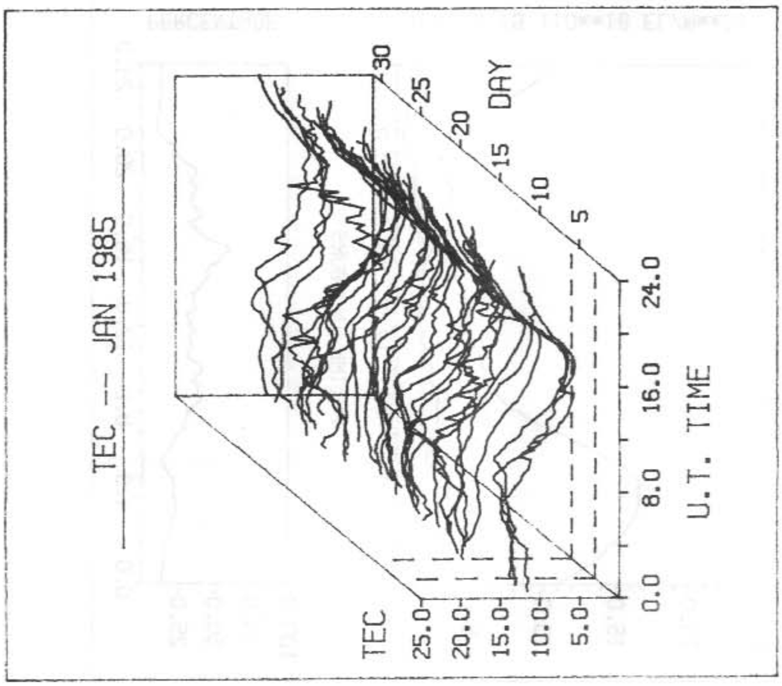
TEC -- JAN 1985
TEC
25.0
20.0
15.0
10.0
5.0
0.0
8.0
16.0
24.0
U.T. TIME
5
10
15
20
25
30
DAY

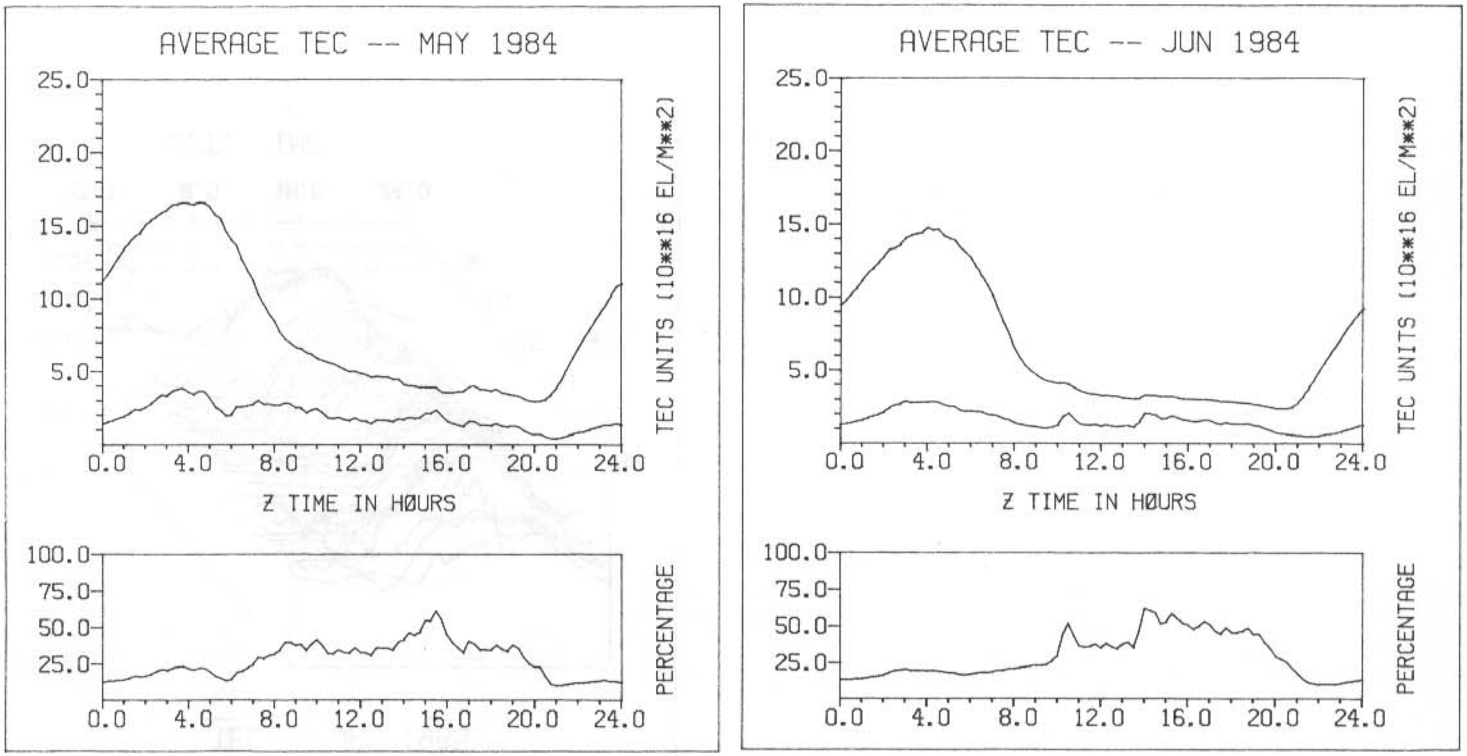

Figure 6. Plots of the monthly average TEC, together with the standard deviation, plotted at 15-minute intervals, and in the lower plot, the ratio as a percentage of the standard deviation to the average value, as an indicator of TEC variability.

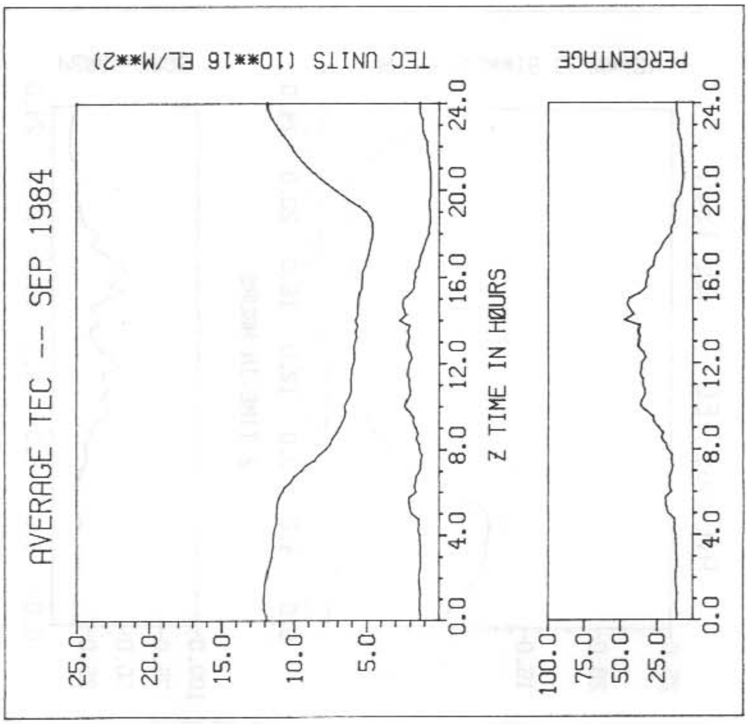
AVERAGE TEC -- SEP 1984
TEC UNITS (10**16 EL/M**2)
25.0
20.0
15.0
10.0
5.0
0.0
4.0
8.0
12.0
16.0
20.0
24.0
Z TIME IN HØURS
PERCENTAGE
100.0
75.0
50.0
25.0

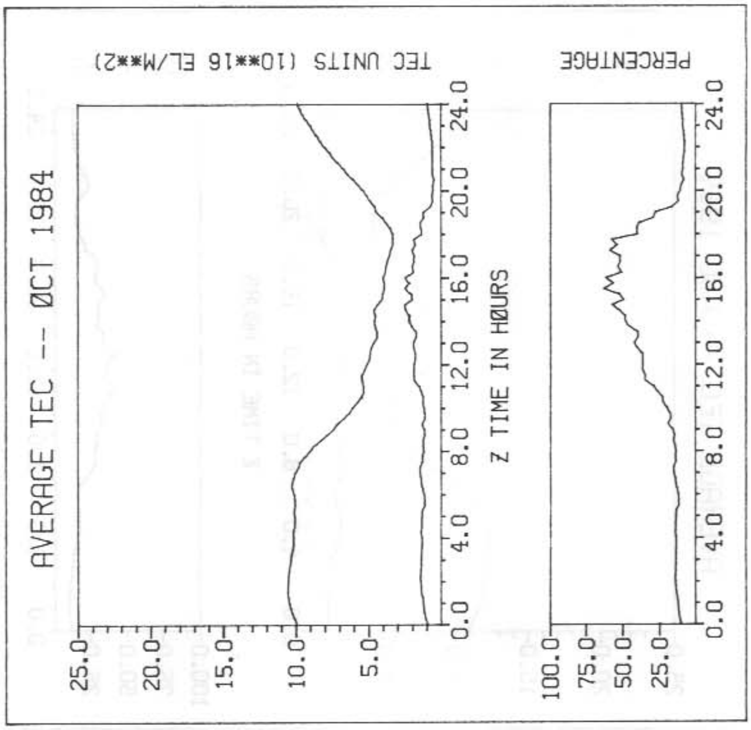
AVERAGE TEC -- ØCT 1984
TEC UNITS (10**16 EL/M**2)
25.0
20.0
15.0
10.0
5.0
0.0
4.0
8.0
12.0
16.0
20.0
24.0
Z TIME IN HØURS
PERCENTAGE
100.0
75.0
50.0
25.0

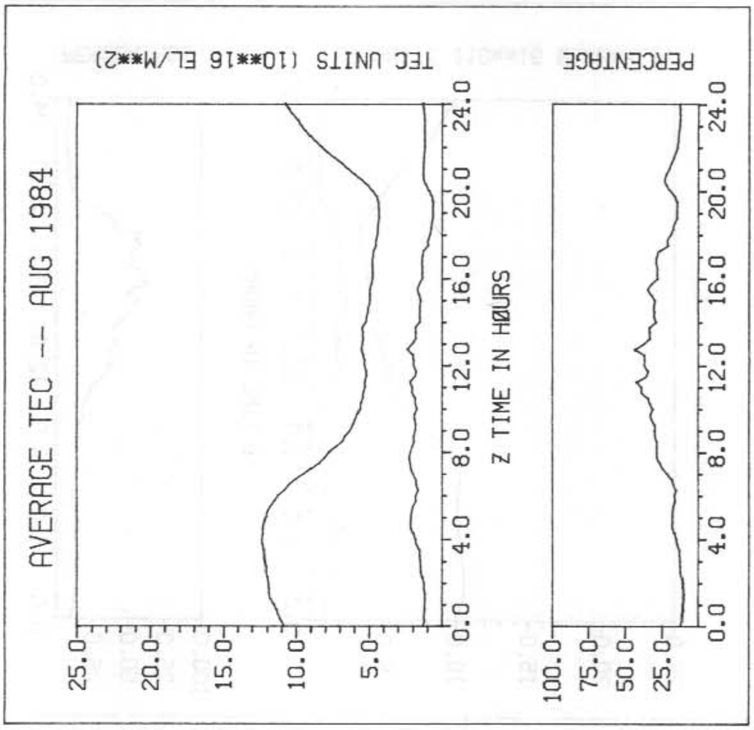
AVERAGE TEC -- AUG 1984
TEC UNITS (10**16 EL/M**2)
25.0
20.0
15.0
10.0
5.0
0.0
4.0
8.0
12.0
16.0
20.0
24.0
Z TIME IN HØURS
PERCENTAGE
100.0
75.0
50.0
25.0

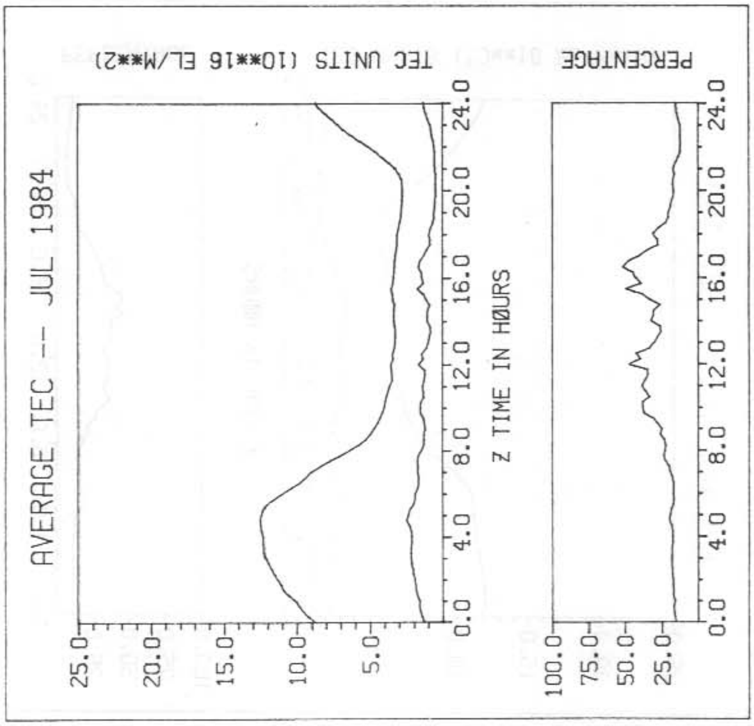
AVERAGE TEC -- JUL 1984
TEC UNITS (10**16 EL/M**2)
25.0
20.0
15.0
10.0
5.0
0.0
4.0
8.0
12.0
16.0
20.0
24.0
Z TIME IN HØURS
PERCENTAGE
100.0
75.0
50.0
25.0

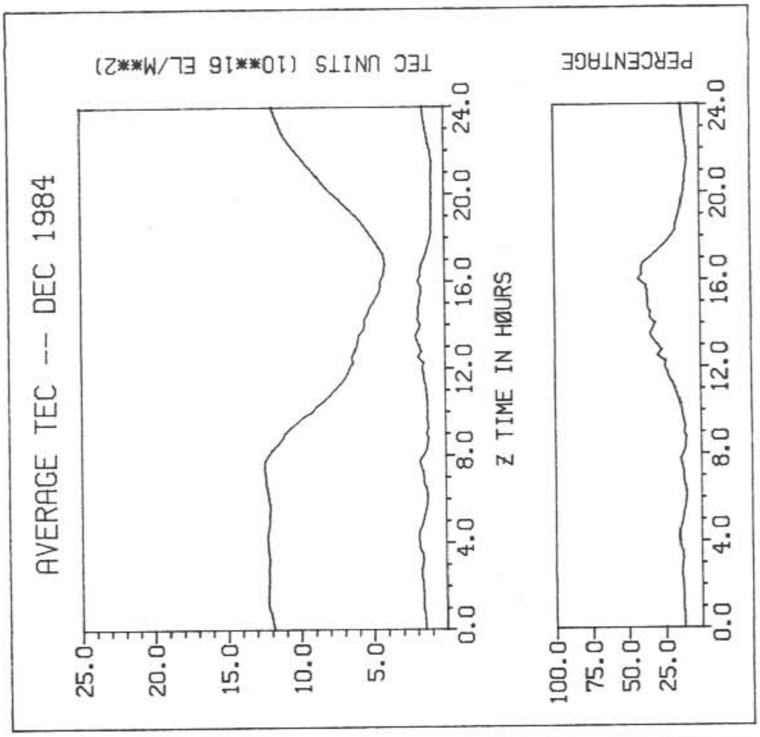
AVERAGE TEC -- DEC 1984
TEC UNITS (10**16 EL/M**2)
25.0
20.0
15.0
10.0
5.0
0.0
4.0
8.0
12.0
16.0
20.0
24.0
Z TIME IN HØURS
PERCENTAGE
100.0
75.0
50.0
25.0

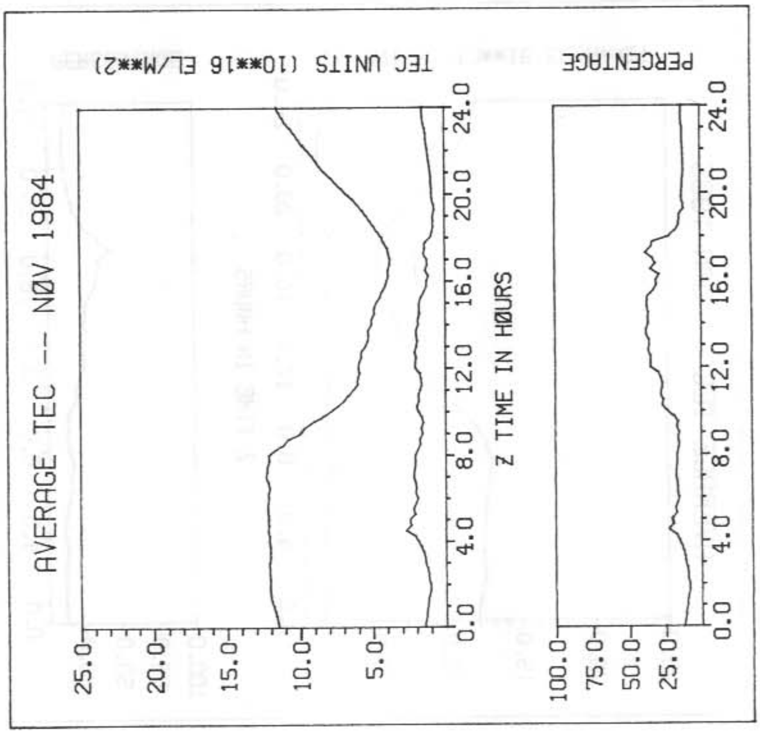
AVERAGE TEC -- NØV 1984
TEC UNITS (10**16 EL/M**2)
25.0
20.0
15.0
10.0
5.0
0.0
4.0
8.0
12.0
16.0
20.0
24.0
Z TIME IN HØURS
PERCENTAGE
100.0
75.0
50.0
25.0

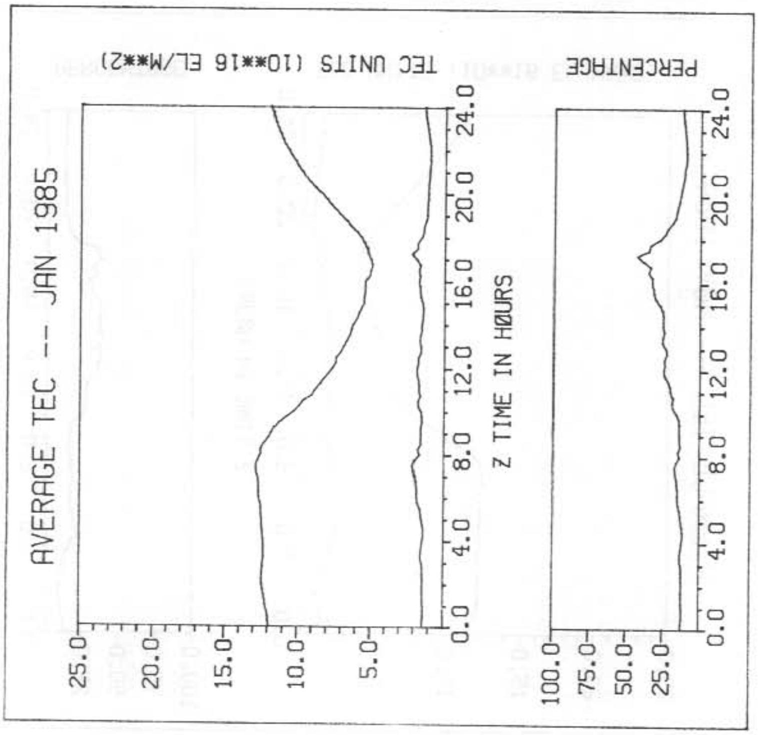

AVERAGE TEC -- JAN 1985
TEC UNITS (10**16 EL/M**2)
PERCENTAGE
Z TIME IN HØURS
25.0
20.0
15.0
10.0
5.0
100.0
75.0
50.0
25.0
0.0
4.0
8.0
12.0
16.0
20.0
24.0

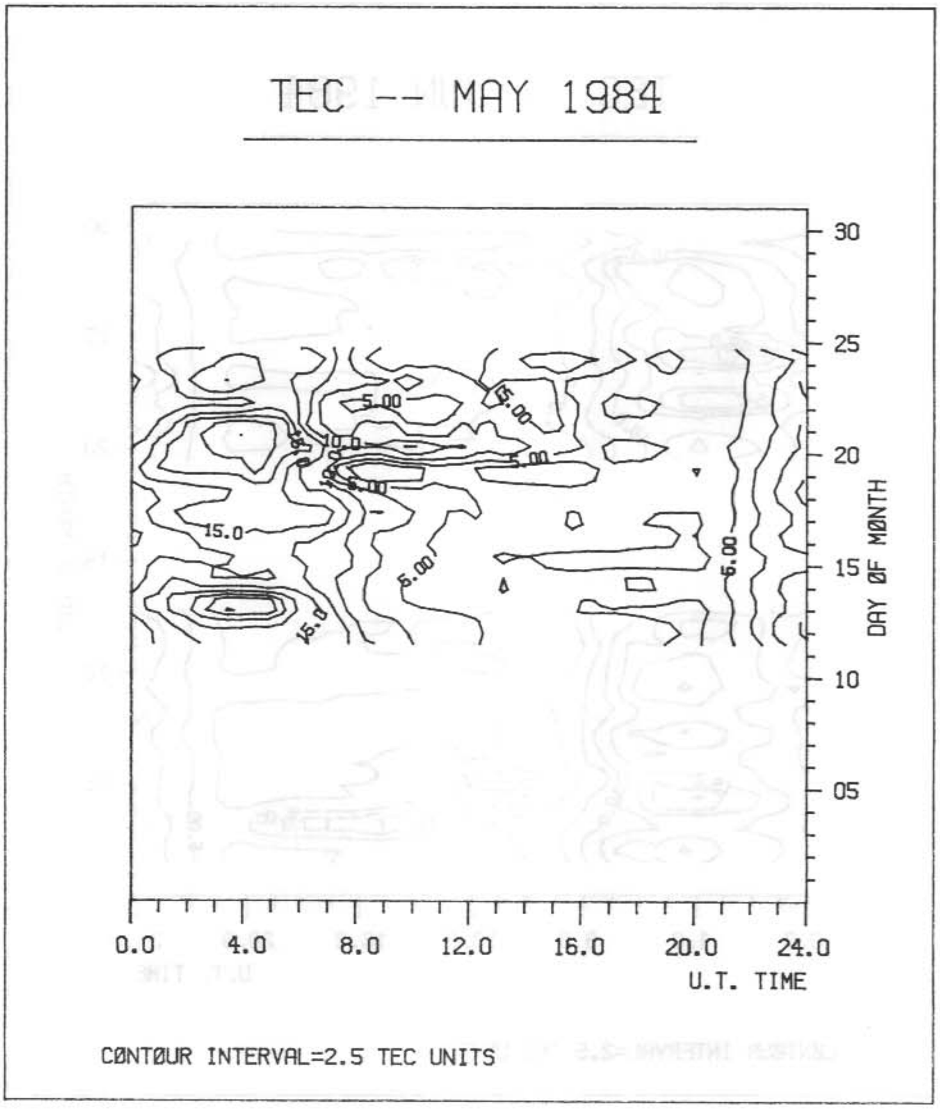

Figure 7. Iso-TEC contours plotted as a function of day-of-month and universal time for each of the 9 months of data collection from May 1984 to January 1985.

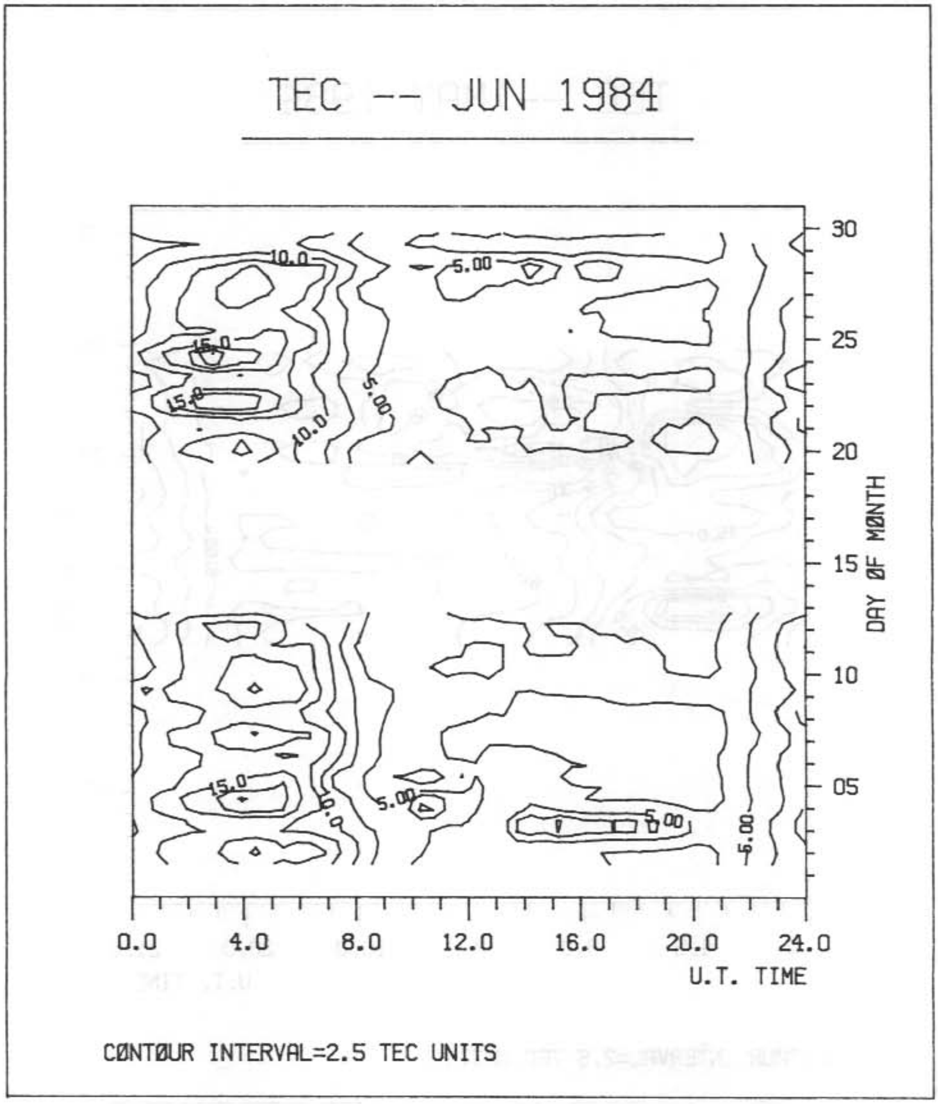

TEC -- JUN 1984
10.0
5.00
15.0
15.0
5.00
10.0
15.0
10.0
5.00
5.00
5.00
30
25
20
15
10
05
DAY ØF MØNTH
0.0
4.0
8.0
12.0
16.0
20.0
24.0
U.T. TIME
CØNTØUR INTERVAL=2.5 TEC UNITS

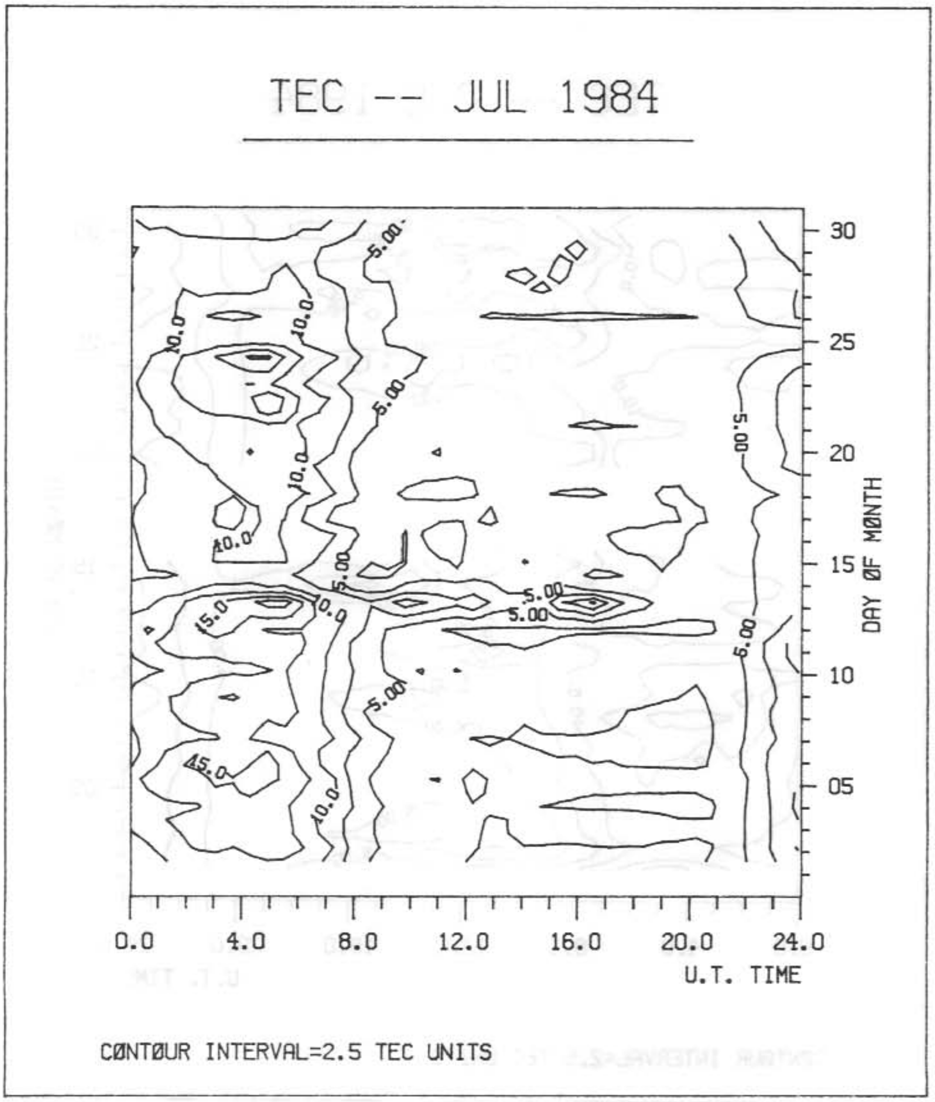

TEC -- JUL 1984
0.0
4.0
8.0
12.0
16.0
20.0
24.0
U.T. TIME
30
25
20
15
10
05
DAY ØF MØNTH
5.00
10.0
15.0
CØNTØUR INTERVAL=2.5 TEC UNITS

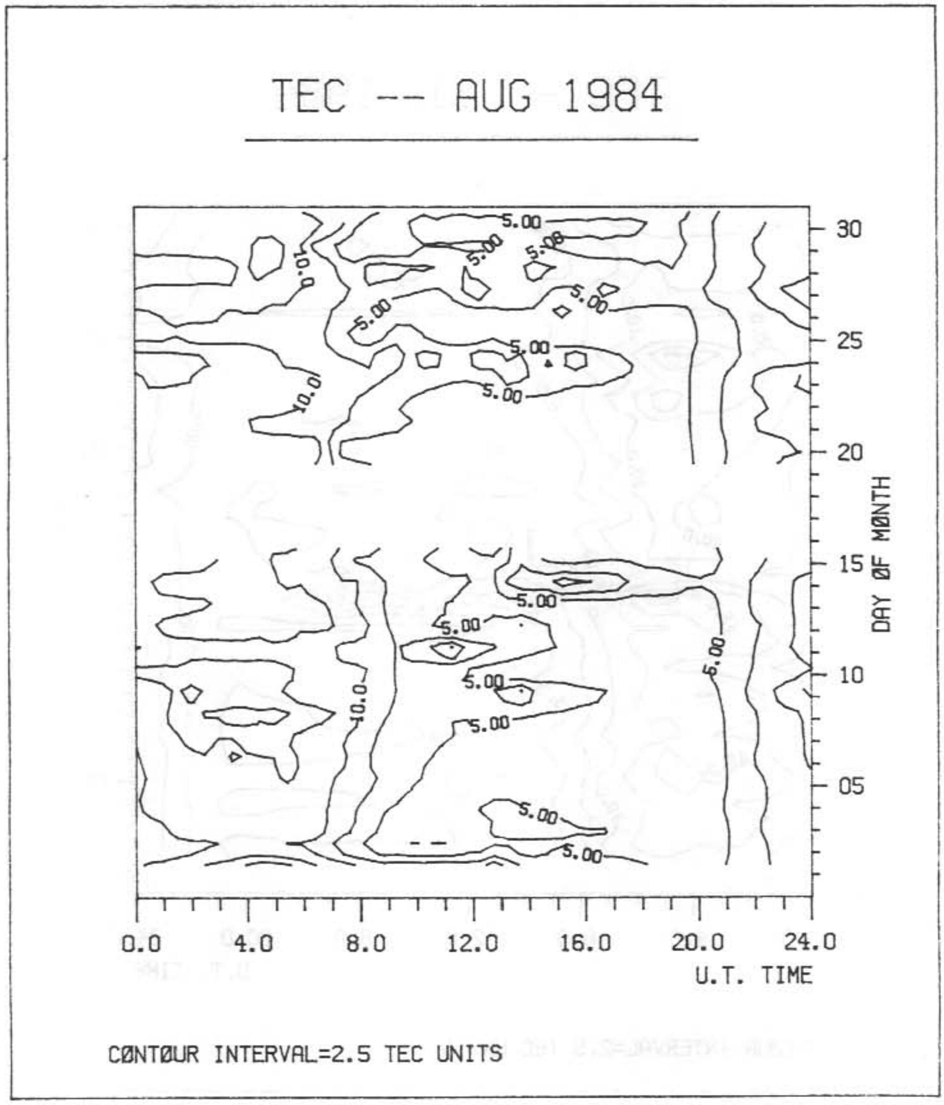
TEC -- AUG 1984
5.00
10.0
DAY ØF MØNTH
30
25
20
15
10
05
0.0
4.0
8.0
12.0
16.0
20.0
24.0
U.T. TIME
CØNTØUR INTERVAL=2.5 TEC UNITS

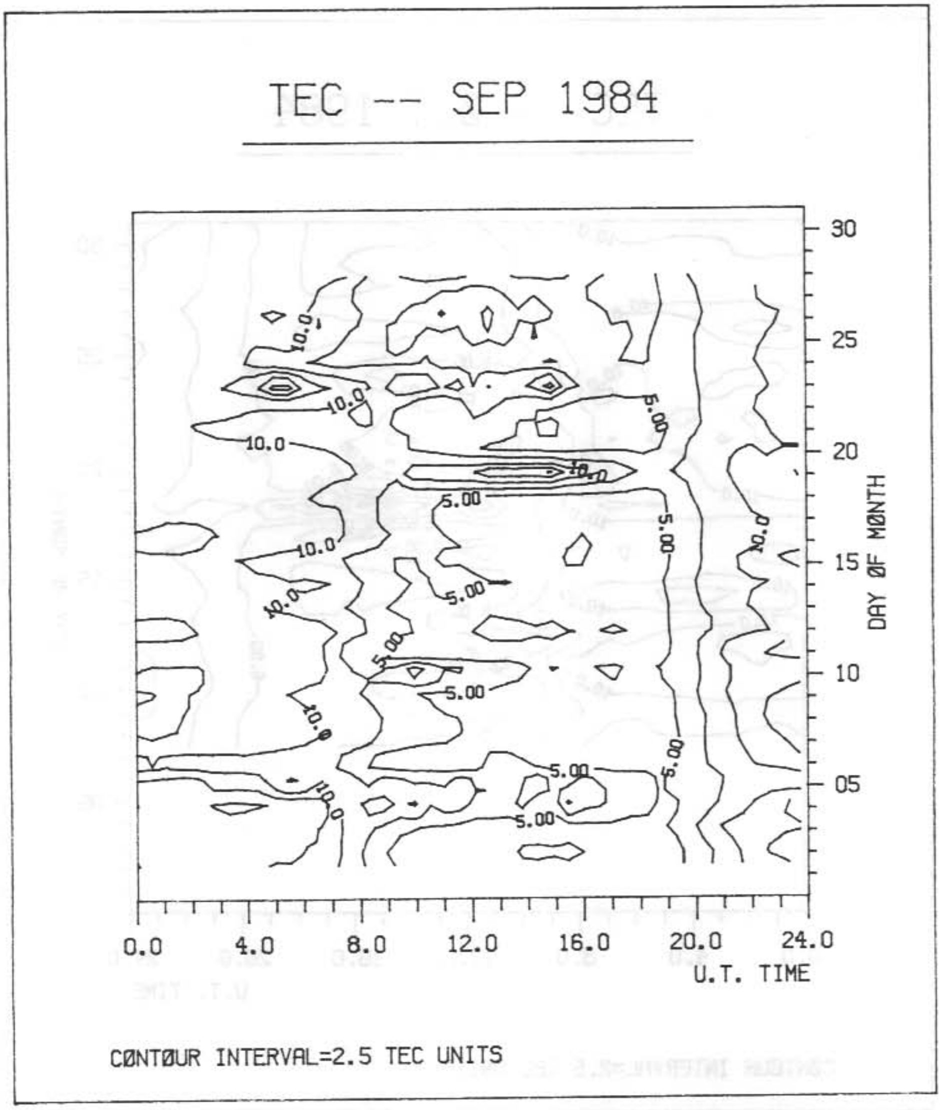
TEC -- SEP 1984
30
25
20
15
10
05
DAY ØF MØNTH
0.0
4.0
8.0
12.0
16.0
20.0
24.0
U.T. TIME
10.0
5.00
CØNTØUR INTERVAL=2.5 TEC UNITS

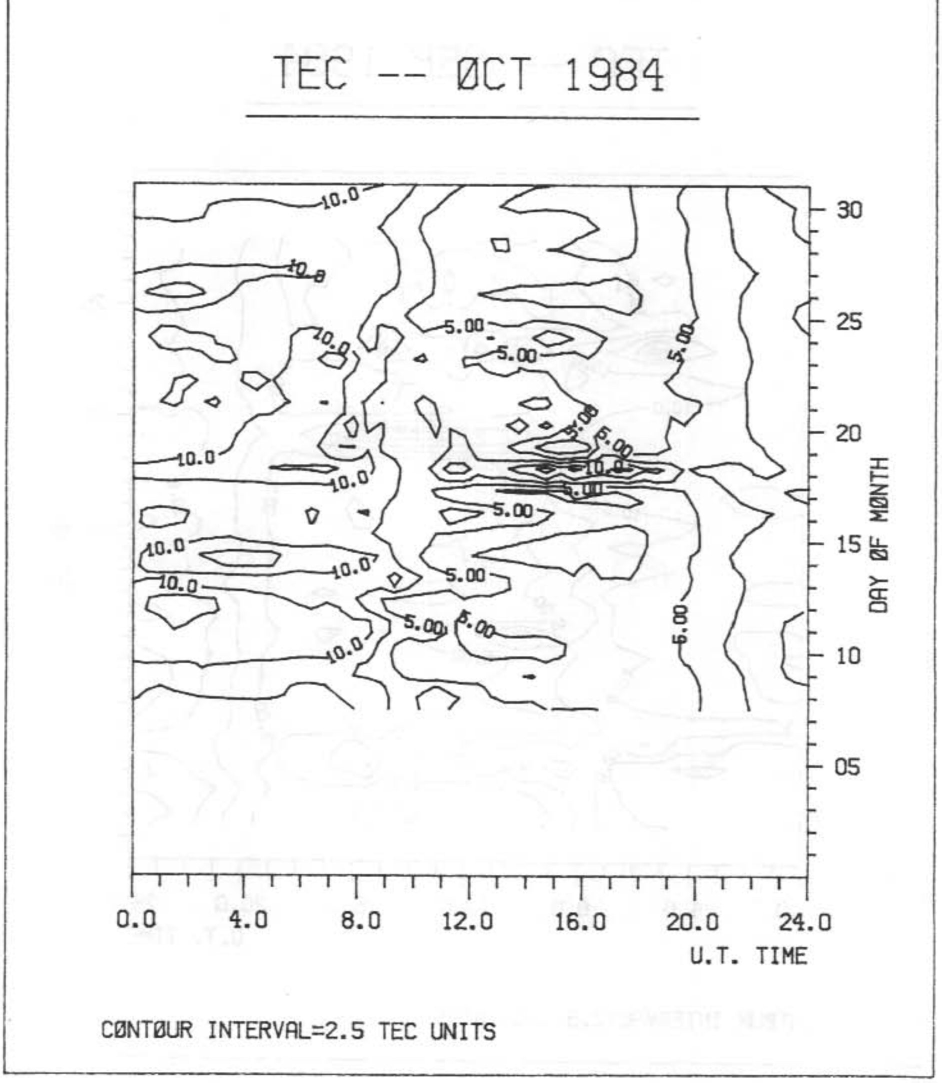

TEC -- ØCT 1984
10.0
5.00
DAY ØF MØNTH
U.T. TIME
0.0
4.0
8.0
12.0
16.0
20.0
24.0
30
25
20
15
10
05
CØNTØUR INTERVAL=2.5 TEC UNITS

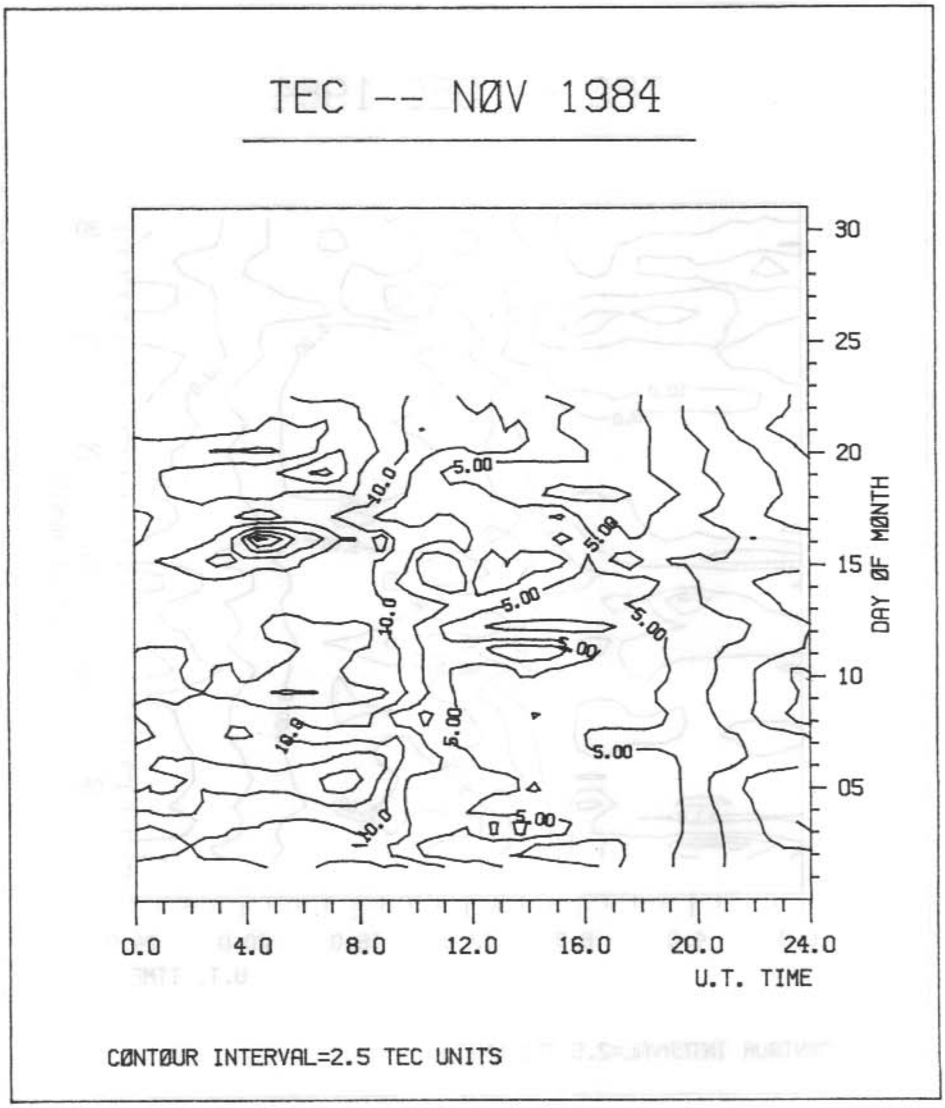

TEC -- NØV 1984
30
25
20
15
10
05
DAY ØF MØNTH
0.0
4.0
8.0
12.0
16.0
20.0
24.0
U.T. TIME
10.0
5.00
CØNTØUR INTERVAL=2.5 TEC UNITS

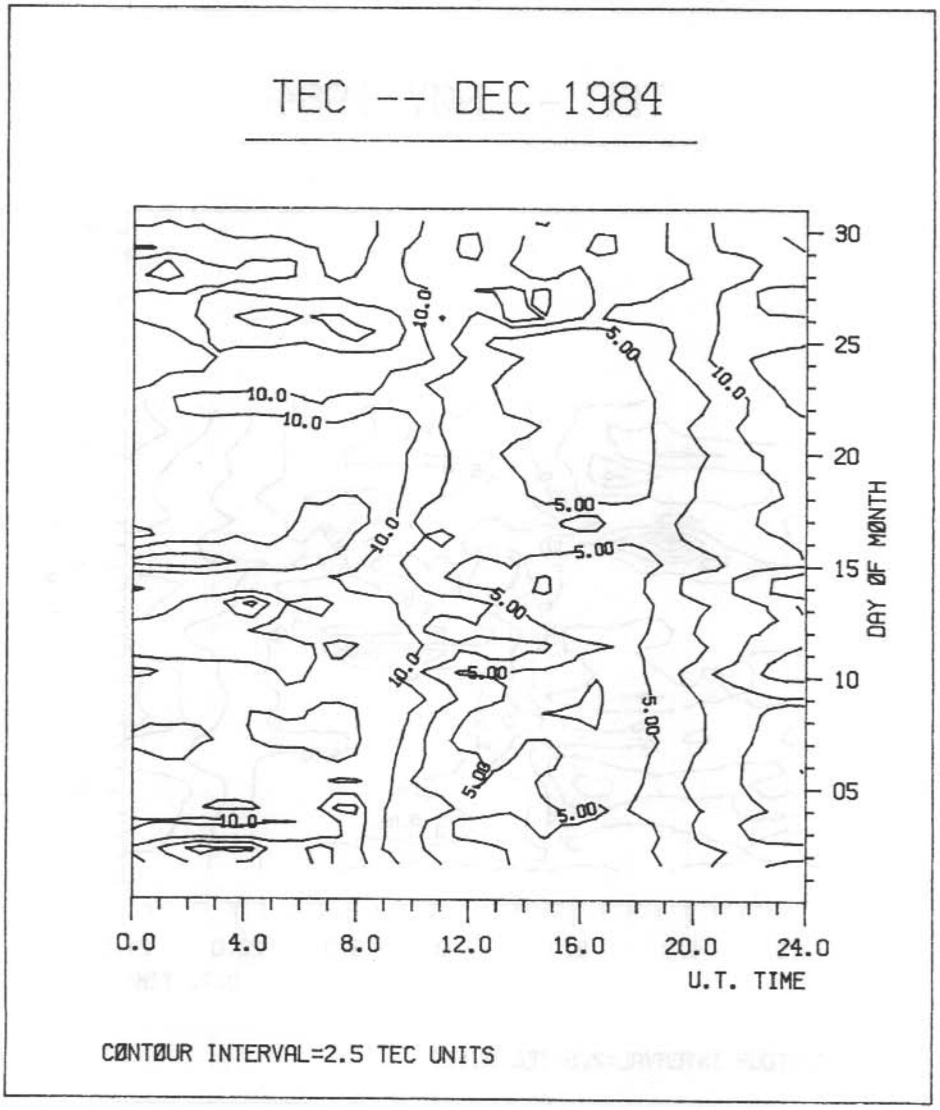

TEC -- DEC 1984
10.0
5.00
30
25
20
15
10
05
DAY ØF MØNTH
0.0
4.0
8.0
12.0
16.0
20.0
24.0
U.T. TIME
CØNTØUR INTERVAL=2.5 TEC UNITS

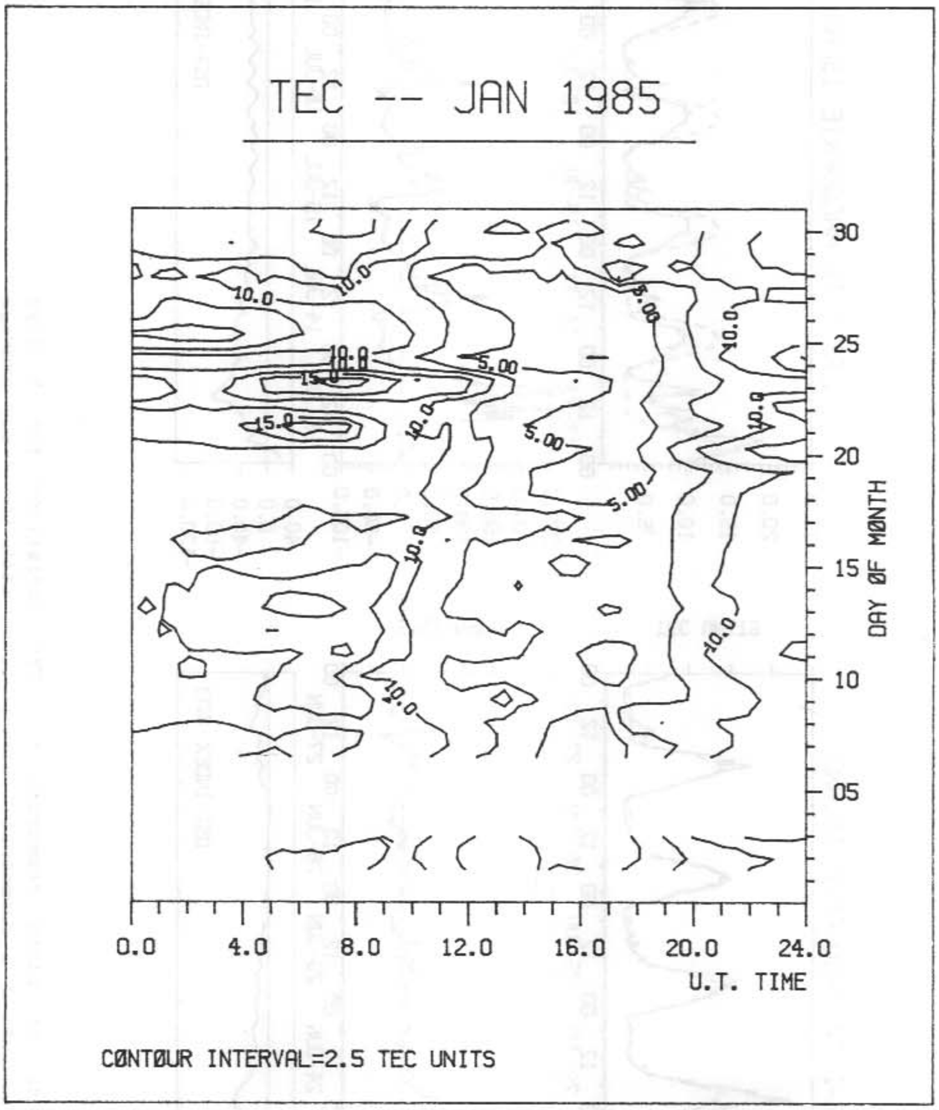

TEC -- JAN 1985
10.0
15.0
5.00
DAY ØF MØNTH
30
25
20
15
10
05
0.0
4.0
8.0
12.0
16.0
20.0
24.0
U.T. TIME
CØNTØUR INTERVAL=2.5 TEC UNITS

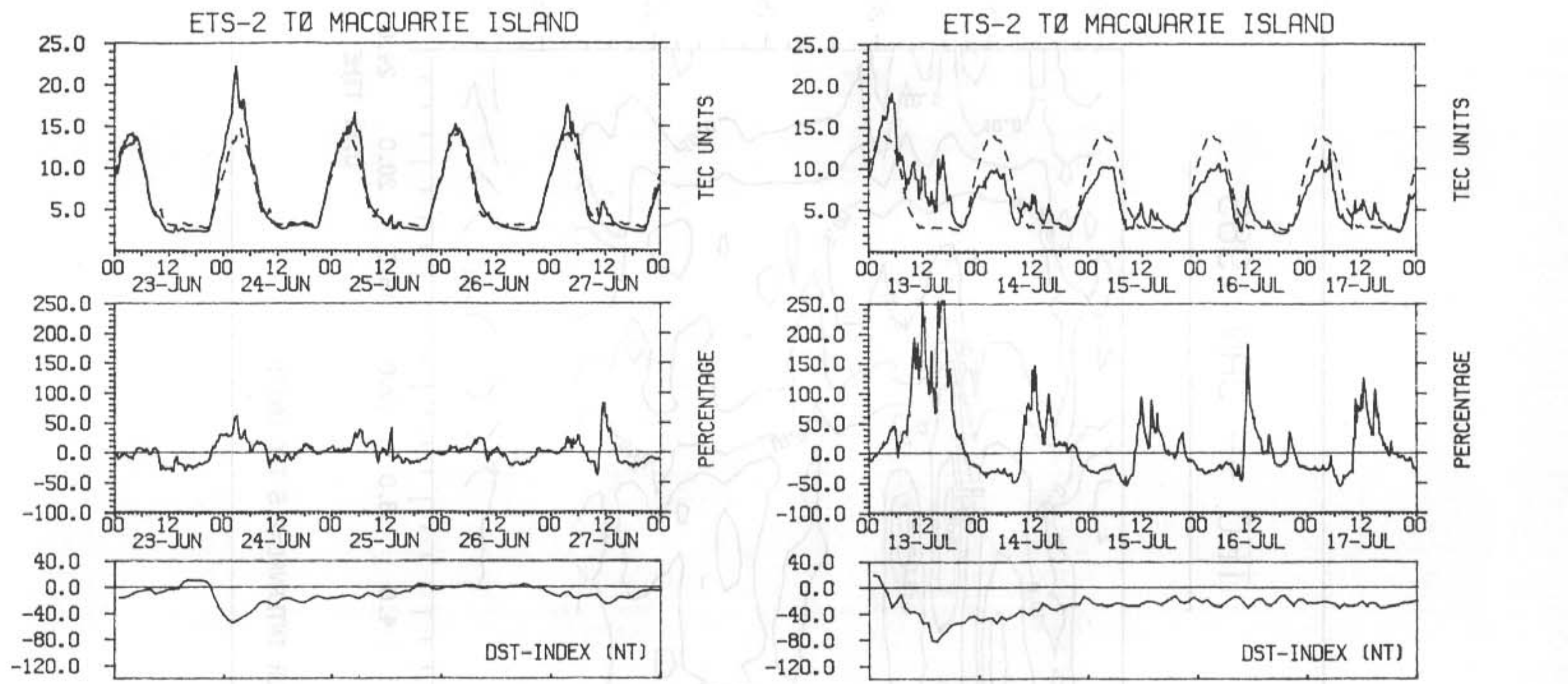

Figure 8. Storm-time plots comparing the TEC variations for 5 days following commencement of a geomagnetic storm event, with the 7-day average TEC level prior to the event. The middle plot displays the percentage change in TEC, and the lower plot gives the Dst-index for the same period.

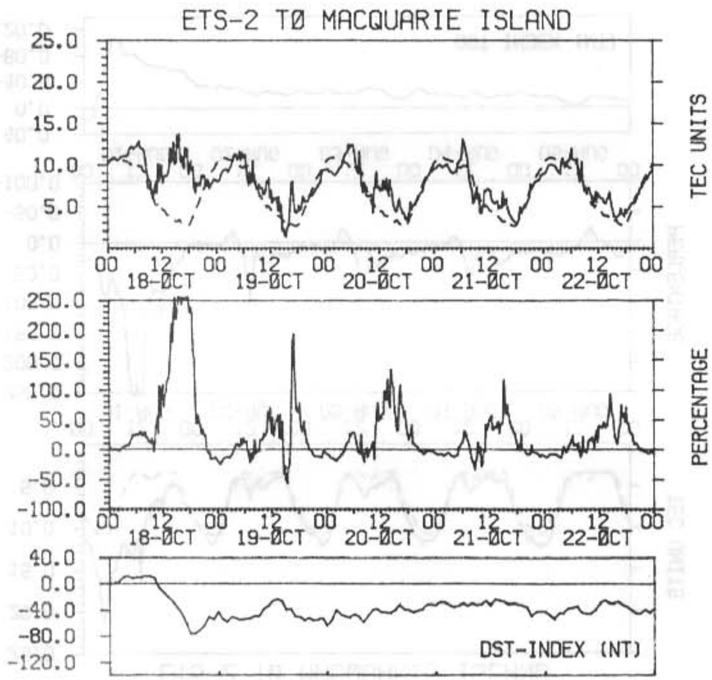
ETS-2 TØ MACQUARIE ISLAND
TEC UNITS
PERCENTAGE
DST-INDEX (NT)
18-ØCT
19-ØCT
20-ØCT
21-ØCT
22-ØCT

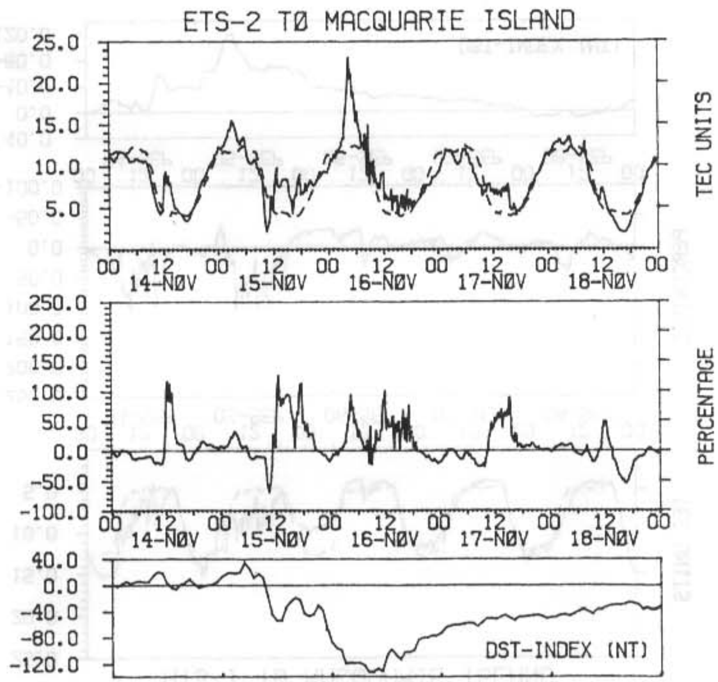
ETS-2 TØ MACQUARIE ISLAND
TEC UNITS
PERCENTAGE
DST-INDEX (NT)
14-NØV
15-NØV
16-NØV
17-NØV
18-NØV

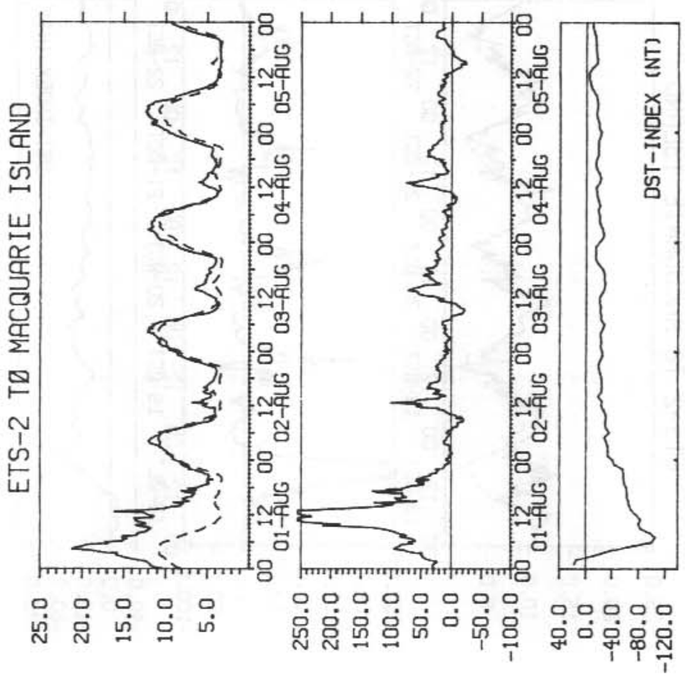
ETS-2 TØ MACQUARIE ISLAND
TEC UNITS
PERCENTAGE
DST-INDEX (NT)
01-AUG
02-AUG
03-AUG
04-AUG
05-AUG

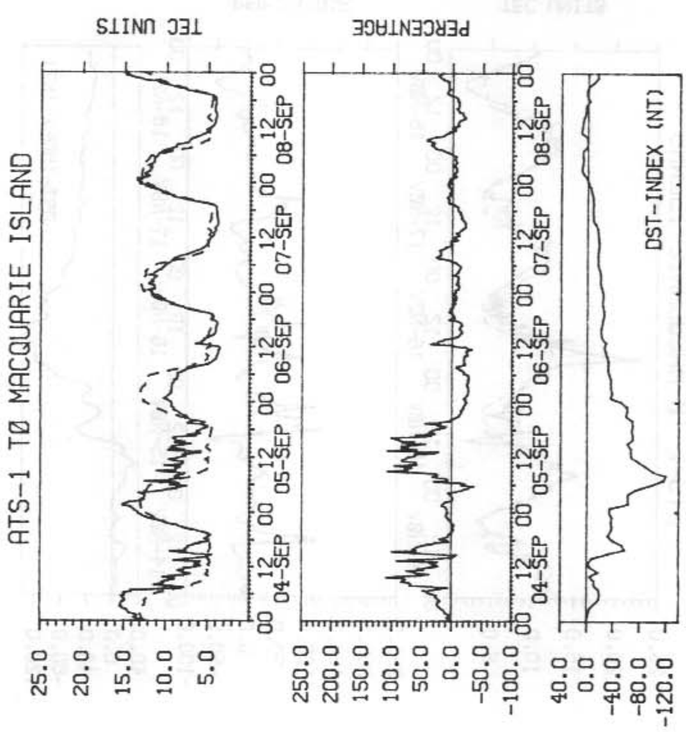
ATS-1 TØ MACQUARIE ISLAND
TEC UNITS
PERCENTAGE
DST-INDEX (NT)
04-SEP
05-SEP
06-SEP
07-SEP
08-SEP

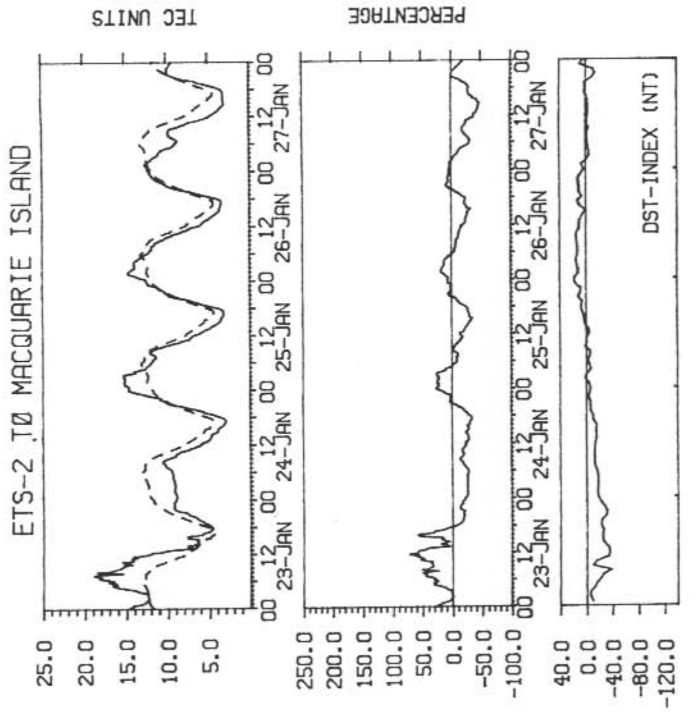
ETS-2 TØ MACQUARIE ISLAND
TEC UNITS
PERCENTAGE
DST-INDEX (NT)
23-JAN
24-JAN
25-JAN
26-JAN
27-JAN

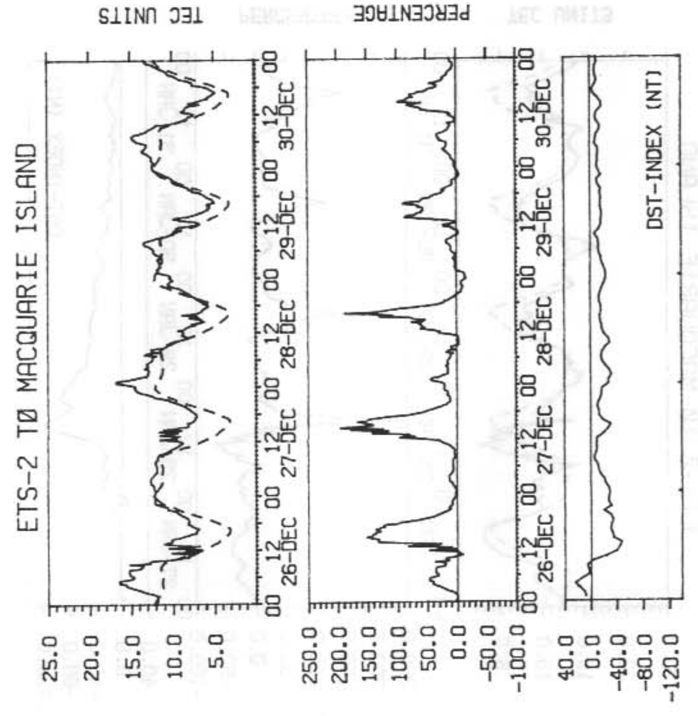
ETS-2 TØ MACQUARIE ISLAND
TEC UNITS
PERCENTAGE
DST-INDEX (NT)
26-DEC
27-DEC
28-DEC
29-DEC
30-DEC

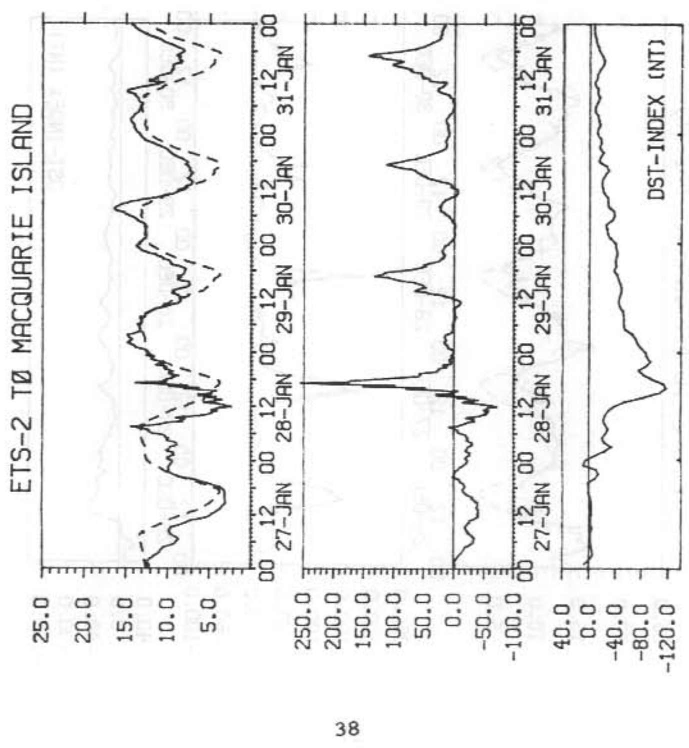
ETS-2 TØ MACQUARIE ISLAND
TEC UNITS
PERCENTAGE
DST-INDEX (NT)
25.0
20.0
15.0
10.0
5.0
250.0
200.0
150.0
100.0
50.0
0.0
-50.0
-100.0
40.0
0.0
-40.0
-80.0
-120.0
00
12
27-JAN
00
12
28-JAN
00
12
29-JAN
00
12
30-JAN
00
12
31-JAN
00

REFERENCES

Checcacci, P.F. and de Giorgio, M.T. (1976). Note on the calibration of T.E.C curves from geostationary satellites. Journal of Atmospheric and Terrestrial Physics 38:219-221.

Davies, K. (1969). Ionospheric Radio Waves. Blaisdell Publishing Company, Waltham, Massachusetts.

Duncan, R.A. (1969). F-region seasonal and magnetic storm behaviour. Journal of Atmospheric and Terrestrial Physics 31:59-70.

Essex, E.A. (1986). The effect of magnetic storms on the ionosphere during 1978. Proceedings of Beacon Satellite Symposium 1:187-200. Oulu, Finland.

Jones, K.L. (1971). Storm time variation of F2-layer electron concentration. Journal of Atmospheric and Terrestrial Physics 33:379-389.

Jones, K.L. and Rishbeth, H. (1971). The origin of storm increases of mid-latitude F-layer electron concentration. Journal of Atmospheric and Terrestrial Physics 33:391-401.

Lambert, M. and Cohen, E.A. (1986). Monitoring ionospheric irregularities in the southern auroral region by means of a satellite beacon. Radio Science 21(3):347-350.

Lambert, M., Jacklyn, P. and Cohen, E.A. (1986). Total electron content of the ionosphere north of Macquarie Island ANARE Research Notes Number 34. Antarctic Division, Kingston.

Lawrence, R.S., Posakony, D.J., Garriott, O.K. and Hall, S.C. (1963). The total electron content of the ionosphere at middle latitudes near the peak of the solar cycle. Journal of Geophysical Research 68(7):1889-1898.

Martyn, D.F. (1953). The morphology of the ionospheric variations associated with magnetic disturbance 1. Variations at moderately low latitudes. Proceedings of the Royal Society 218(A):1-18.

Matsushita, S. (1959). A study of the morphology of ionospheric storms. Journal of Geophysical Research 64(3):305-321.

Mendillo, M. (1973). A study of the relationship between geomagnetic storms and ionospheric disturbances at mid-latitudes. Planetary and Space Science 21:349-358.

Peddie, N.W. (1982). International Geomagnetic Reference Field: the third generation. Journal of Geomagnetism and Geoelectricity 34: 309-326.

Seaton, M.J. (1956). A possible explanation of the drop in F critical densities accompanying major ionospheric storms Journal of Atmospheric and Terrestrial Physics 8:122-124.

Smith, D.H. (1971). Removal of the nΠ ambiguity in observations of total electron content. Journal of Atmospheric and Terrestrial Physics 33:1161-1168.

Soicher, H. (1986). Variability of transionospheric signal time delay at subauroral latitudes. IEEC Transactions on Antennas and Propagation AP-34(110):1313-1319.

Taylor, G.N. (1965). Integrated electron production and loss rates in the ionosphere. Planetary and Space Science 13:507-520.

Titheridge, J.E. (1966). Continuous records of the total electron content of the ionosphere. Journal of Atmospheric and Terrestrial Physics 28:1135-1150.

Yeh, K.C. and Swenson, G.W. (1961). Ionospheric electron content and its variations deduced from satellite observations. Journal of Geophysical Research 66:1061-1067.

Zmuda, A.J. (1971). IGRF (1965.0). World Magnetic Survey 1957-1969. IAGA Bulletin No 28. Pp. 186-188. IUGG Publications.

ACKNOWLEDGMENTS

The data were collected at the ANARE station on Macquarie Island. Equipment and technical backup for the data collection and reduction was provided by the La Trobe University Division of Theoretical and Space Physics, and by the Upper Atmospheric Physics Section of the Antarctic Division. The authors would like to thank David Watts (Antarctic Division) and Michael Mallis (LaTrobe University) for their assistance with computer software, and the Ionospheric Prediction Service for the provision of Macquarie Island and Hobart foF2 data. Finance for this research was provided by the Antarctic Science Advisory Committee grants scheme. Special thanks also to Dr Gary Burns (Antarctic Division) and Dr Phil Wilkinson (Ionospheric Prediction Service) for their very helpful advice with the manuscript.